Check for updates

New Phytologist

Research

BRASSINOSTEROID-SIGNALING KINASE 1 phosphorylating CALCIUM/CALMODULIN-DEPENDENT PROTEIN KINASE functions in drought tolerance in maize

Lei Liu[1,2], Yang Xiang[1], Jingwei Yan[1,3], Pengcheng Di[1], Jing Li[1], Xiujuan Sun[1], Gaoqiang Han[1], Lan Ni[1,3], Mingyi Jiang[1,3], Jianhua Yuan[2] and Aying Zhang[1,3]

[1]College of Life Sciences, Nanjing Agricultural University, Nanjing 210095, China; [2]Institute of Food Crops, Provincial Key Laboratory of Agrobiology, Jiangsu Academy of Agricultural Sciences, Nanjing 210014, China; [3]National Key Laboratory of Crop Genetics and Germplasm Enhancement, Nanjing Agricultural University, Nanjing 210095, China

Author for correspondence:
Aying Zhang
Email: ayzhang@njau.edu.cn

Received: *25 January 2021*
Accepted: *6 April 2021*

New Phytologist (2021) **231:** 695–712
doi: 10.1111/nph.17403

Key words: drought tolerance, maize, transphosphorylation, ZmBSK1, ZmCCaMK.

Summary

- Drought stress seriously limits crop productivity. Although studies have been carried out, it is still largely unknown how plants respond to drought stress. Here we find that drought treatment can enhance the phosphorylation activity of brassinosteroid-signaling kinase 1 (ZmBSK1) in maize (*Zea mays*).
- Our genetic studies reveal that ZmBSK1 positively affects drought tolerance in maize plants. ZmBSK1 localizes in plasma membrane, interacts with calcium/calmodulin (Ca^{2+}/CaM)-dependent protein kinase (ZmCCaMK), and phosphorylates ZmCCaMK. Ser-67 is a crucial phosphorylation site of ZmCCaMK by ZmBSK1.
- Drought stress enhances not only the interaction between ZmBSK1 and ZmCCaMK but also the phosphorylation of Ser-67 in ZmCCaMK by ZmBSK1. Furthermore, Ser-67 phosphorylation in ZmCCaMK regulates its Ca^{2+}/CaM binding, autophosphorylation and transphosphorylation activity, and positively affects its function in drought tolerance in maize.
- Our results reveal an important role for ZmBSK1 in drought tolerance and suggest a direct regulatory mode of ZmBSK1 phosphorylating ZmCCaMK.

Introduction

Drought stress is one of the major abiotic stresses that limits crop productivity (Porcel *et al.*, 2003; Boutraa *et al.*, 2010; Chai *et al.*, 2016). During long-term evolution, plants have developed mechanisms to protect themselves from stress damage. Antioxidant defense systems, such as antioxidant defense enzymes superoxide dismutase (SOD), ascorbate peroxidase (APX), catalase (CAT) and glutathione reductase (GR), can scavenge excess reactive oxygen species (ROS) caused by drought stress and protect plants from oxidative damage (Farooq *et al.*, 2009; Xia *et al.*, 2009; Zhang *et al.*, 2010; Anjum *et al.*, 2011; Ahammed *et al.*, 2013; Xu *et al.*, 2013; Hayat *et al.*, 2014; Vardhini & Anjum, 2015; Kaya *et al.*, 2019). Previous studies suggested that protein kinases, such as calcium/calmodulin-dependent protein kinase (CCaMK) and mitogen-activated protein kinase (MAPK), positively regulate the responses of plants to drought stress by inducing antioxidant defense system (Ma *et al.*, 2012; Shi *et al.*, 2012; Zhu *et al.*, 2016; Ni *et al.*, 2019). However, the mechanism by which plants cope with drought stress is unclear.

Calcium/calmodulin-dependent protein kinase is a plant-specific protein kinase, which is characterized by a N-terminal kinase domain, a calmodulin (CaM)-binding domain (CBD) and a visinin-like domain (VLD) containing three Ca^{2+}-binding EF-hands in C-terminal (Mitra *et al.*, 2004; Singh & Parniske, 2012; Miller *et al.*, 2013; Poovaiah *et al.*, 2013). Ca^{2+}-stimulated autophosphorylation increases the affinity of CCaMK to Ca^{2+}/CaM (Sathyanarayanan *et al.*, 2000), resulting in the activation of transphosphorylation. The roles of CCaMK have been well studied in both arbuscular mycorrhizal symbiosis (AMS) and root nodule symbiosis (RNS) (Levy *et al.*, 2004; Gleason *et al.*, 2006; Tirichine *et al.*, 2006; Hayashi *et al.*, 2010; Shimoda *et al.*, 2012; Takeda *et al.*, 2012; Miller *et al.*, 2013; Jin *et al.*, 2016). CCaMK interacts with and phosphorylates the Interacting Protein of DMI3 (IPD3)/CYCLOPS transcription factor to activate nodulation process (Yano *et al.*, 2008; Kang *et al.*, 2011; Singh *et al.*, 2014; Pimprikar *et al.*, 2016; Diedhiou & Diouf, 2018). More and more studies show that CCaMK is also involved in the responses of plants to abiotic stresses (Pandey *et al.*, 2002; C. Yang *et al.*, 2010; L. Yang *et al.*, 2010; Shi *et al.*, 2012; Zhu *et al.*, 2016; Ni *et al.*, 2019). In *Arabidopsis*, overexpressing *Triticum aestivuml CCaMK* (*TaCCaMK*) not only improves the tolerance to salt stress during seed germination but also reduces sensitivity to abscisic acid (ABA) (C. Yang *et al.*, 2010). Recently, biochemical and genetic analyses have shown that *Oryza sativa* CCaMK, OsDMI3, positively regulates the tolerance of plants to water stress and oxidative stress (Ni *et al.*, 2019). In maize, ZmCCaMK phosphorylating NAC84 regulates

© 2021 The Authors
New Phytologist © 2021 New Phytologist Foundation

ABA-induced antioxidant defense and drought stress (Zhu *et al.*, 2016). However, how CCaMK responds to drought stress remains largely unknown.

Here, we identify *Zea mays* brassinosteroid-signaling kinase 1 (ZmBSK1) as an interaction protein of ZmCCaMK. Brassinosteroid-signaling kinases belong to the subfamily of receptor-like cytoplasmic kinases (RLCK-XII) containing an N-terminal kinase domain and a C-terminal tetratricopeptide repeat (TPR) domain (Shiu *et al.*, 2004; Kim & Wang, 2010). Twelve BSK proteins are identified in *Arabidopsis*. BSK1, BSK2 and BSK3 are BR-responsive proteins (Tang *et al.*, 2008). BSK1 plays an important role in the BR signaling pathway (Nolan *et al.*, 2020). BSK1 is phosphorylated by brassinosteroid-insensitive 1 (BRI1) and then dissociates from the receptor complex to activate BRI1-suppressor 1 (BSU1). Activated BSU1 dephosphorylates and inhibits brassinosteroid-insensitive 2 (BIN2), which leads to dephosphorylation of two transcription factors, brassinazole-resistant 1 (BZR1) and BRI1 EMS suppressor 1 (BES1/BZR2), by the protein phosphatase 2A (PP2A). Dephosphorylated BZR1 and BES1 accumulate in the nucleus and regulate BR-responsive gene expression. BSK1 and BSK2 are also involved in the embryonic YODA (YDA) pathway and the ERECTA family/YDA pathway (Neu *et al.*, 2019). Brassinosteroid-signaling kinases are required for normal plant growth and development, and functional overlap exists among BSK3, BSK4, BSK6, BSK7 and BSK8 (Tang *et al.*, 2008; Sreeramulu *et al.*, 2013; Zhang *et al.*, 2016; Jia *et al.*, 2019; Ren *et al.*, 2019).

Moreover, BSK family members also function in plant immunity (Shi *et al.*, 2013; Wang *et al.*, 2017; Majhi *et al.*, 2019). BSK1 interacts with the immune receptor FLS2 and phosphorylates MAPKKK5 to regulate immunity (Shi *et al.*, 2013; Yan *et al.*, 2018). OsBSK1-2 regulates flg22- and chitin-triggered immune responses in rice plants (Wang *et al.*, 2017). BSK5 functions in pattern-triggered immunity by interacting with immune receptors (Majhi *et al.*, 2019). In addition to the roles in plant immunity, BSKs also respond to abiotic stress. Li *et al.* (2012) reported that *Arabidopsis* loss-of-function mutant *bsk5* exhibits sensitivity to salinity and ABA, and BSK5 is required for salt stress and ABA-mediated drought stress tolerance. Recent studies show that barley *BSK2* is downregulated in XZ5 (drought-tolerant) under drought treatment (Chen *et al.*, 2019), while *Populus tomentosa BSK* is upregulated under cold stress (Yang *et al.*, 2019). These findings suggest that BSKs play important roles in regulating multiple physiological processes. However, the mechanisms by which BSKs function in plants in response to abiotic stresses remain unclear. Here, we demonstrate that ZmBSK1-mediated phosphorylation of ZmCCaMK plays an important role in regulating the tolerance of maize plants to drought stress.

Materials and Methods

Plant materials and treatment

Maize (*Zea mays* L.) inbred line B73 and tobacco (*Nicotiana benthamiana* L.) were used in this study. Maize seeds were sown on pots containing sterile soil mixture (soil : vermiculite, 1 : 1, v/v) in a growth chamber at a temperature of 25°C, photosynthetic active radiation of 200 $\mu mol\ m^{-2}\ s^{-1}$ and photoperiod 14 h : 10 h, light : dark, and were watered daily. For protoplast isolation, maize plants were grown at 25°C under dark conditions until the second leaves were fully expanded.

For polyethylene glycol (PEG) treatment, 10-d-old seedlings were excised at the base of stem and placed in distilled water for 2 h to eliminate wound stress, then placed in beakers wrapped with aluminum foil containing distilled water or 10% (w/v) PEG6000 solutions for various lengths of time. After PEG treatment, the second leaves were sampled and used for further analysis.

GST pull-down assay

Glutathione S-transferase (GST) and GST-ZmBSK1 were expressed in *E. coli* BL21 (DE3), and bacteria were lysed in lysis buffer (137 mM NaCl, 2.7 mM KCl, 4.3 mM Na_2HPO_4, 1.4 mM KH_2PO_4, pH 7.4). After centrifugation at 4°C for 20 min, the soluble proteins were incubated with MagneGST glutathione particles (Promega) with gentle rotation at 4°C for 1 h. After washing three times with MagneGST wash buffer (140 mM NaCl, 10 mM KCl, 4.2 mM Na_2HPO_4, 2 mM KH_2PO_4, pH 7.2), the particles were incubated with purified His-ZmCCaMK in MagneGST binding buffer (140 mM NaCl, 10 mM KCl, 4.2 mM Na_2HPO_4, 2 mM KH_2PO_4, 10% (w/v) BSA (Solarbio, Beijing, China), pH 7.2) with gentle rotation at 4°C for 1 h. The particles were washed three times with MagneGST wash buffer and boiled in sodium dodecyl sulfate (SDS) loading buffer. Samples were separated on 12% SDS-polyacrylamide gel electrophoresis (SDS-PAGE) and analyzed by immunoblotting with monoclonal anti-His or monoclonal anti-GST antibody (Abmart, Shanghai, China).

Coimmunoprecipitation assay

For tobacco leaves transformation system, the full-length coding sequence of *ZmCCaMK*, *ZmBSK1* and *ZmCaM1* was introduced into vector 1300-221-3*Flag or 1300-221-6*Myc driven by cauliflower mosaic virus 35S promoter. The constructs were transiently expressed in 4-wk-old tobacco leaves by *Agrobacterium tumefaciens* strain GV3101 infiltration. After 3 d of infiltration, total proteins were extracted from leaves using lysis buffer (10 mM Tris-HCl, pH 7.5, 150 mM NaCl, 5 mM EDTA, 1% (v/v) Triton X-100, 0.1% (w/v) SDS, 0.5 mM dithiothreitol (DTT), and plant protease inhibitor cocktail). Protein extracts (200 μg) were immunoprecipitated with monoclonal anti-Flag antibody (1 : 300; Abmart) bound to protein A/G agarose in immunoprecipitation buffer (20 mM Tris-HCl, pH 7.5, 20 mM KCl, 150 mM NaCl, 10 mM $MgCl_2$ and plant protease inhibitor cocktail) at 4°C for 8 h. The agarose was washed three times with immunoprecipitation buffer and boiled in SDS loading buffer. After centrifugation, the supernatants were separated on 12% SDS-PAGE and analyzed by immunoblotting with monoclonal anti-Myc antibody (Abmart).

For 10-d-old maize seedlings, the detached plants were treated with or without 10% (w/v) PEG6000 solutions for 90 min. Total

© 2021 The Authors
New Phytologist © 2021 New Phytologist Foundation

14698137, 2021, 2, Downloaded from https://nph.onlinelibrary.wiley.com/doi/10.1111/nph.17403 by Zhejiang Agr & For University, Wiley Online Library on [17/10/2023]. See the Terms and Conditions (https://onlinelibrary.wiley.com/terms-and-conditions) on Wiley Online Library for rules of use; OA articles are governed by the applicable Creative Commons License

14698137, 2021, 2, Downloaded from https://nph.onlinelibrary.wiley.com/doi/10.1111/nph.17403 by Zhejiang Agr & For University, Wiley Online Library on [17/10/2023]. See the Terms and Conditions (https://onlinelibrary.wiley.com/terms-and-conditions) on Wiley Online Library for rules of use; OA articles are governed by the applicable Creative Commons License

proteins were extracted from leaves using lysis buffer (10 mM Tris-HCl, pH 7.5, 150 mM NaCl, 5 mM EDTA, 1% (v/v) Triton X-100, 0.1% (w/v) SDS, 0.5 mM DTT, and plant protease inhibitor cocktail). Protein extracts (200 μg) were immunoprecipitated with anti-ZmCCaMK antibody (10 μg; Abmart) bound to protein A/G agarose in immunoprecipitation buffer at 4°C for 8 h. The agarose was washed three times with immunoprecipitation buffer and boiled in SDS loading buffer. After centrifugation, the supernatants were separated on 12% SDS-PAGE and analyzed by immunoblotting with anti-ZmBSK1 antibody (Abmart).

Firefly luciferase complementation imaging (LCI) assay

The full-length coding sequence of *ZmCCaMK* and *ZmBSK1* was introduced into vector pCAMBIA1300-cLUC and pCAMBIA1300-nLUC driven by cauliflower mosaic virus 35S promoter, respectively. The N-terminal fragment of luciferase (nLUC) was fused with ZmBSK1, and the C-terminal fragment of luciferase (cLUC) was fused with ZmCCaMK. These constructs were transformed into *Agrobacterium* strain GV3101 and infiltrated into 4-wk-old tobacco leaves. Firefly luciferase complementation imaging assay was performed as described previously (Chen *et al.*, 2008). After 3 d of infiltration, 1 mM D-luciferin (Sigma-Aldrich) was sprayed onto the leaves and kept for 20 min in the dark, and then the LUC image was captured by a low-light cooled charge coupled device camera (Tanon 5200 Multi, Shanghai, China).

Isolation of total RNA and qRT-PCR analysis

Total RNA was isolated from maize leaves using RNAiso Plus Kit (TaKaRa, Beijing, China) according to the manufacturer's protocol and the cDNA was synthesized using 5×All-In-One MasterMix with AccuRT Genomic DNA Removal Kit (abm, Zhenjiang, China). Real-time quantitative reverse transcription polymerase chain reaction (RT-PCR) was performed on a CFX96 Touch (Bio-Rad) system using EvaGreen 2×qPCR MasterMix-No Dye (abm) according to the manufacturer's protocol. The primers are shown in Supporting Information Table S1. The expression level was normalized against that of *ZmActin2*.

Immunoprecipitation kinase assay and *in vitro* kinase assay

Proteins were extracted from maize leaves as described previously (Ma *et al.*, 2012). Protein content was measured according to the method of Bradford (1976) with bovine serum albumin (BSA; Solarbio) as standard. The anti-ZmCCaMK antibody was raised against the full length of ZmCCaMK, and was purified from serum of immunized rabbits. The anti-ZmBSK1 antibody was raised against the full length of ZmBSK1, and was purified from serum of immunized rabbits. Both of them were generated by biotech company Abmart. Protein extracts (200 μg) were incubated with polyclonal anti-ZmBSK1 antibody (10 μg) or polyclonal anti-ZmCCaMK antibody (10 μg) bound to protein A/G agarose beads in an immunoprecipitation buffer according to Zhang *et al.* (2006). Kinase activity in the immunocomplex was determined by a gel kinase assay using myelin basic protein (MBP; Sigma-Aldrich) as substrate. For ZmBSK1, 1 μg MBP was incubated with immunoprecipitated ZmBSK1 in kinase reaction buffer (25 mM Tris-HCl, pH 7.5, 15 mM NaCl, 1 mM DTT, 5 mM $MnCl_2$ and 10 μCi [γ-^{32}P]ATP (Perkin-Elmer, Waltham, MA, USA)) at 30°C for 30 min. For ZmCCaMK, 1 μg MBP was incubated with immunoprecipitated ZmCCaMK in kinase reaction buffer (25 mM Tris-HCl, pH 7.5, 15 mM NaCl, 1 mM DTT, 5 mM $MgCl_2$, 1 mM $CaCl_2$, 1 μM CaM (Sigma-Aldrich) and 10 μCi [γ-^{32}P]ATP (Perkin-Elmer)) at 30°C for 30 min.

For an *in vitro* kinase assay, purified GST-ZmBSK1, His-ZmCCaMK and various mutant proteins were used. A quantity of 5 μg GST-ZmBSK1 or its mutant proteins were incubated with 10 μg His-ZmCCaMK or its mutant proteins or 1 μg MBP in kinase reaction buffer (25 mM Tris-HCl, pH 7.5, 15 mM NaCl, 1 mM DTT, 5 mM $MgCl_2$ or $MnCl_2$, 1 mM $CaCl_2$, 1 μM CaM (Sigma-Aldrich) and 10 μCi [γ-^{32}P]ATP (Perkin-Elmer)) at 30°C for 30 min. Reactions were stopped by the addition of SDS loading buffer and the reaction mixtures were separated on 12% SDS-PAGE. The unincorporated [γ-^{32}P]ATP was removed by washing with trichloroacetic acid (TCA) buffer containing 5% (w/v) TCA and 1% (w/v) sodium pyrophosphate at least three times. The gel was dried and exposed to autoradiography. Signals were detected by a Typhoon 9410 phosphor imager (Amersham Biosciences, Piscataway, NJ, USA).

LC-MS/MS analysis

To prepare samples for MS analysis, 5 μg GST-ZmBSK1 were incubated with 10 μg His-ZmCCaMK in kinase reaction buffer (25 mM Tris-HCl, pH 7.5, 15 mM NaCl, 1 mM DTT, 5 mM $MnCl_2$, 1 mM $CaCl_2$ and 100 nM ATP) at 30°C for 30 min. His-ZmCCaMK (10 μg) was incubated in kinase reaction buffer (25 mM Tris-HCl, pH 7.5, 15 mM NaCl, 1 mM DTT, 5 mM $MgCl_2$, 1 mM $CaCl_2$ and 100 nM ATP) at 30°C for 30 min. Reactions were stopped by the addition of SDS loading buffer and the reaction mixtures were separated on 12% SDS-PAGE followed by Coomassie brilliant blue (CBB) staining. The corresponding bands of His-ZmCCaMK were sliced and subjected to in-gel digestion with trypsin (10 ng μl^{-1}; Promega) at 37°C for 16 h. The phosphopeptides were enriched and analyzed using Nano LC-LTQ Orbitrap XL LC-MS/MS System (Thermo Scientific, Waltham, MA, USA) as previously described (Gampala *et al.*, 2007). The MS data were analyzed with Thermo Scientific ProteomeDiscoverer software (v.1.3), and the identified phosphorylated peptides were manually inspected to ensure high confidence in phosphorylation site assignment according to the highest post-translational modification score (Tables S2, S3).

Gel shift assay

The Ca^{2+}-induced mobility shift assay of fusion proteins was performed as described previously (Vallone *et al.*, 2016). A quantity of 10 μg of purified His-ZmCCaMK or its mutant proteins was incubated with 5 mM $CaCl_2$ or 10 mM EGTA in binding buffer (25 mM Tris-HCl, pH 7.5) at 25°C for 15 min. The samples were separated on 12% native PAGE and the gel was stained with CBB.

© 2021 The Authors
New Phytologist © 2021 New Phytologist Foundation

$^{45}Ca^{2+}$ overlay assay

Calmodulin (Sigma-Aldrich), BSA (Solarbio), purified His, purified His-ZmCCaMK and its mutant proteins (5 μg) were spotted on a nitrocellulose membrane (Pall Corporation, Port Washington, NY, USA). The membrane was incubated in binding buffer (20 mM Tris-HCl, pH 7.0, 50 mM KCl) containing 1 μCi $^{45}Ca^{2+}$ (Perkin-Elmer) at room temperature for 20 min. After incubation, the membrane was washed with 50% ethanol three times and exposed to autoradiography. Signals were detected using a Typhoon 9410 phosphor imager (Amersham Biosciences).

CaM-binding assay

Calmodulin-binding assays were performed as described previously with minor modification (Arazi *et al.*, 1995). In brief, the full-length coding sequence of *ZmCaM1* was introduced into vector pGEX-4T-1 for GST-ZmCaM1 fusion protein. Purified His-ZmCCaMK or its mutant proteins were separated on 12% SDS-PAGE and transferred to a polyvinylidene difluoride membrane (Merck Millipore). The membrane was incubated with 15 μg purified GST-ZmCaM1 proteins in binding buffer (10 mM Tris-HCl, pH 7.5, 150 mM NaCl, and 5% (w/v) skimmed milk powder) in the presence of 5 mM $CaCl_2$ or 10 mM EGTA at 4°C for 8 h. After incubation, the membrane was washed with binding buffer without skimmed milk powder at least three times, and was then detected by immunoblotting with anti-GST antibody (Abmart).

Maize transformation and regeneration

The full-length coding sequence of *ZmBSK1*, *ZmCCaMK* or its mutants was introduced into plant expression vector pCUN-NHF driven by *ubiquitin* promoter. The maize inbred line B73 was used as the plant receptor. The *Agrobacterium*-mediated maize shoot-tip transformation was performed as described by Liu *et al.* (2015) with minor modifications; the transformation efficiency improved from 2% to *c.* 8% after the following optimization. In brief, these constructs were transformed into *Agrobacterium* strain LBA4404, and the bacteria were suspended in distilled water containing 150 μM acetosyringone (Sigma-Aldrich) to OD_{600} at 0.65. The injured maize shoot tips (exposed meristems) were soaked in the bacterial suspension for 3 min at a pressure of 0.05 MPa, and cultured in sterile soil mixture (soil : vermiculite, 1 : 1, v/v) in the dark at 25°C. After 3 d in the dark, the plants were grown routinely in the light. Positive transformants were selected by spraying with 75 mg l^{-1} herbicide Basta (Sangon Biotech, Shanghai, China), and were then further confirmed by PCR amplification. Resistant T_2 seedlings with 3 : 1 segregation of resistance were transferred to soil to obtain homozygous T_3 seeds from individual lines.

Phenotype and oxidative damage analysis

For the growth phenotype, 10-d-old maize seedlings were subjected to progressive drought by withholding water for 6 or 8 d and then rewatered and recovered for 3 d after which the survival rates were counted. For the analysis of oxidative damage, 10-d-old maize seedlings were subjected to progressive drought by withholding water for 2 d; the content of malondialdehyde (MDA) and the percentage of electrolyte leakage were measured as described by Shi *et al.* (2012).

Antioxidant defense enzyme assay

The maize leaves were homogenized in 0.6 ml of 50 mM potassium phosphate buffer (pH 7.0) containing 1 mM EDTA and 1% (w/v) polyvinylpyrrolidone 40. The homogenate was centrifuged at 12 000 ***g*** for 30 min at 4°C and the supernatant was used for the subsequent antioxidant defense enzyme assays. Total activities of antioxidant defense enzymes (SOD and APX) were measured as described previously (Zhu *et al.*, 2016).

Statistical analysis

Statistical analysis was performed using the software SPSS 16.0 (https://www.ibm.com/products/spss-statistics). One-way or two-way ANOVA corrected with Duncan's multiple range test was used to determine statistical significance. Differences were considered significant at $P < 0.05$.

Results

ZmCCaMK interacts with ZmBSK1

Our previous study showed that ZmCCaMK functioned in the responses of maize to drought stress (Ma *et al.*, 2012; Yan *et al.*, 2015; Zhu *et al.*, 2016). To understand how ZmCCaMK functions, we identified an interaction protein, ZmBSK1. Fluorescence was observed in tobacco leaves injected with ZmBSK1-nLUC and cLUC-ZmCCaMK using firefly luciferase complementation imaging (LCI) assay (Fig. 1a). For bimolecular fluorescence complementation (BiFC) assay, when split yellow fluorescent protein (YFP) ZmBSK1-nYFP was cotransformed with ZmCCaMK-cYFP into maize mesophyll protoplasts, a strong YFP fluorescence signal was observed in the plasma membrane, indicating the physical interaction between ZmBSK1 and ZmCCaMK (Fig. 1b; Methods S1). To further investigate the interaction between ZmBSK1 and ZmCCaMK, we expressed and purified the recombinant GST-ZmBSK1 and His-ZmCCaMK proteins, and then performed glutathione S-transferase (GST) pull-down assay (Methods S2, S3). As shown in Fig. 1(c), His-ZmCCaMK was pulled down by GST-ZmBSK1 but not GST alone, suggesting that ZmBSK1 can interact with ZmCCaMK. Moreover, we also performed a coimmunoprecipitation (Co-IP) assay to confirm the interaction between ZmBSK1 and ZmCCaMK. The fusion constructs of Myc-ZmBSK1 and Flag-ZmCCaMK were introduced into tobacco leaves, and the crude protein extracts from leaves were immunoprecipitated with anti-Flag antibody and then analyzed by immunoblotting with anti-Myc antibody. And the interaction between Myc-ZmBSK1 and Flag-ZmCCaMK was observed (Fig. 1d). To further confirm this interaction in maize, we

© 2021 The Authors
New Phytologist © 2021 New Phytologist Foundation

14698137, 2021, 2, Downloaded from https://nph.onlinelibrary.wiley.com/doi/10.1111/nph.17403 by Zhejiang Agr & For University, Wiley Online Library on [17/10/2023]. See the Terms and Conditions (https://onlinelibrary.wiley.com/terms-and-conditions) on Wiley Online Library for rules of use; OA articles are governed by the applicable Creative Commons License

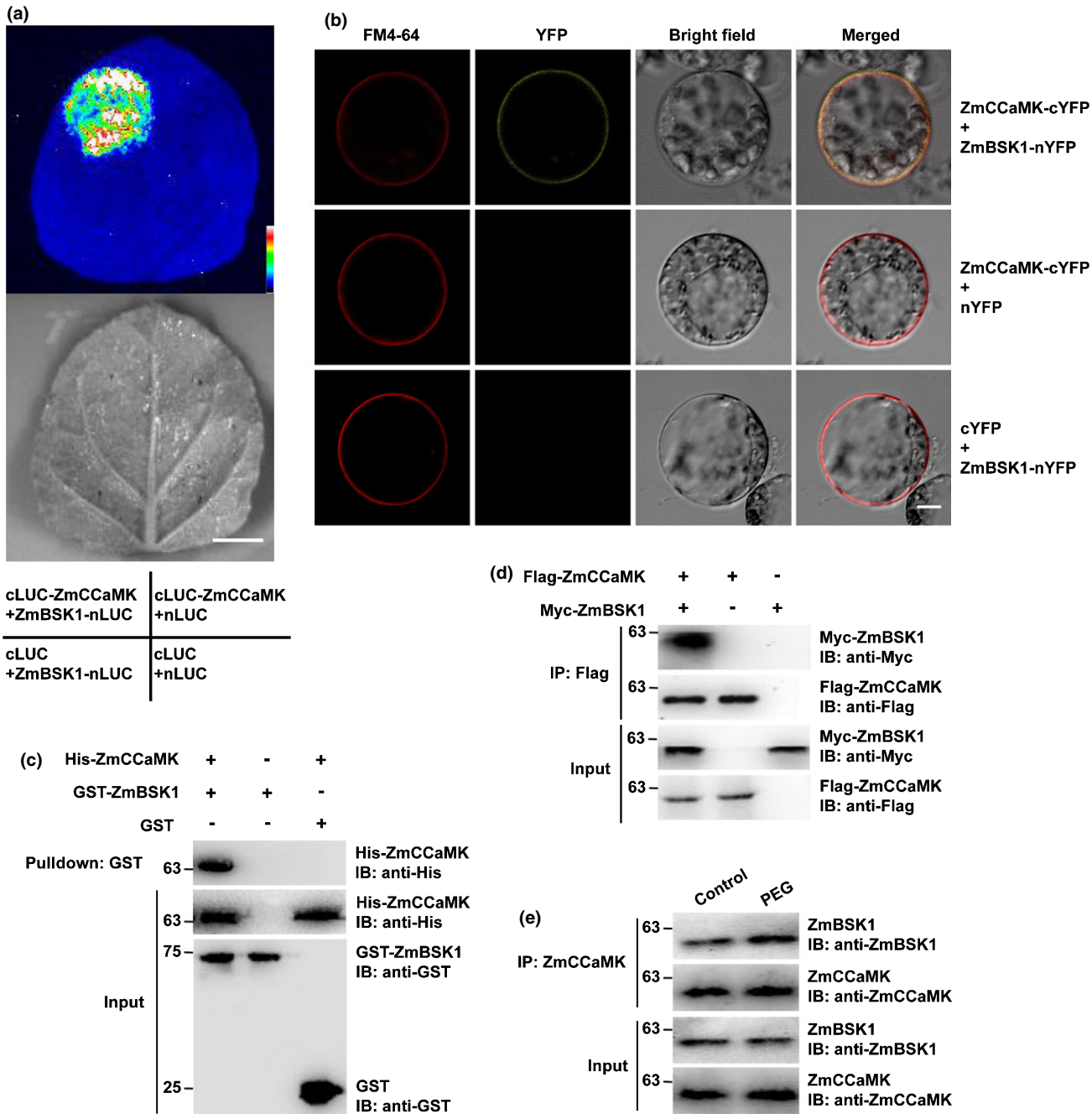

Fig. 1 *Zea mays* calcium/calmodulin-dependent protein kinase (ZmCCaMK) physically interacts with *Zea mays* brassinosteroid-signaling kinase 1 (ZmBSK1) *in vitro* and *in vivo*. (a) Firefly luciferase complementation imaging (LCI) assay. Tobacco (*Nicotiana benthamiana*) leaves were cotransformed with constructs *35S:cLUC-ZmCCaMK* and *35S:ZmBSK1-nLUC*. Combinations of *35S:cLUC-ZmCCaMK* and *35S:nLUC*, *35S:cLUC* and *35S:ZmBSK1-nLUC*, and *35S:cLUC* and *35S:nLUC* constructs were used as negative controls. Image was collected from the detached leaves after infiltration for 3 d. Bar, 1 cm. (b) Bimolecular fluorescence complementation (BiFC) assay. Fusion constructs *35S:ZmCCaMK-cYFP* and *35S:ZmBSK1-nYFP* were transformed into maize protoplasts simultaneously. Combinations of *35S:ZmCCaMK-cYFP* and *35S:nYFP*, and *35S:cYFP* and *35S:ZmBSK1-nYFP* constructs were used as negative controls. The fluorescence signals were visualized under laser confocal microscopy after incubation for 14 h. Plasma membrane was stained with N-[3-triethylammoniumpropyl]-4-[6-(4-(diethylamino) phenyl) hexatrienyl] pyridinium dibromide (FM4-64; red). Bar, 8 μm. (c) Glutathione S-transferase (GST) pull-down assay. Purified His-ZmCCaMK was used to incubate with GST-ZmBSK1 in glutathione particles, and the eluted fractions were detected by immunoblotting with anti-His antibody. GST protein was used as control. (d) Coimmunoprecipitation (Co-IP) assay in tobacco leaves. Fusion constructs *35S:Myc-ZmBSK1* and *35S:Flag-ZmCCaMK* were transiently expressed in tobacco leaves simultaneously or separately. Total protein extracts were immunoprecipitated with anti-Flag antibody. ZmBSK1 and ZmCCaMK were detected by immunoblotting with anti-Myc and anti-Flag antibodies, respectively. (e) Co-IP assay of the effect of polyethylene glycol (PEG) on the interaction between ZmCCaMK and ZmBSK1 in maize leaves. Ten-day-old seedlings were treated with or without 10% PEG6000 for 90 min. Total protein extracts were immunoprecipitated with anti-ZmCCaMK antibody. ZmBSK1 and ZmCCaMK were detected by immunoblotting with anti-ZmBSK1 and anti-ZmCCaMK antibodies, respectively. The molecular weights are marked on the left. All experiments were repeated at least three times with similar results.

© 2021 The Authors
New Phytologist © 2021 New Phytologist Foundation

14698137, 2021, 2, Downloaded from https://nph.onlinelibrary.wiley.com/doi/10.1111/nph.17403 by Zhejiang Agr & For University, Wiley Online Library on [17/10/2023]. See the Terms and Conditions (https://onlinelibrary.wiley.com/terms-and-conditions) on Wiley Online Library for rules of use; OA articles are governed by the applicable Creative Commons License

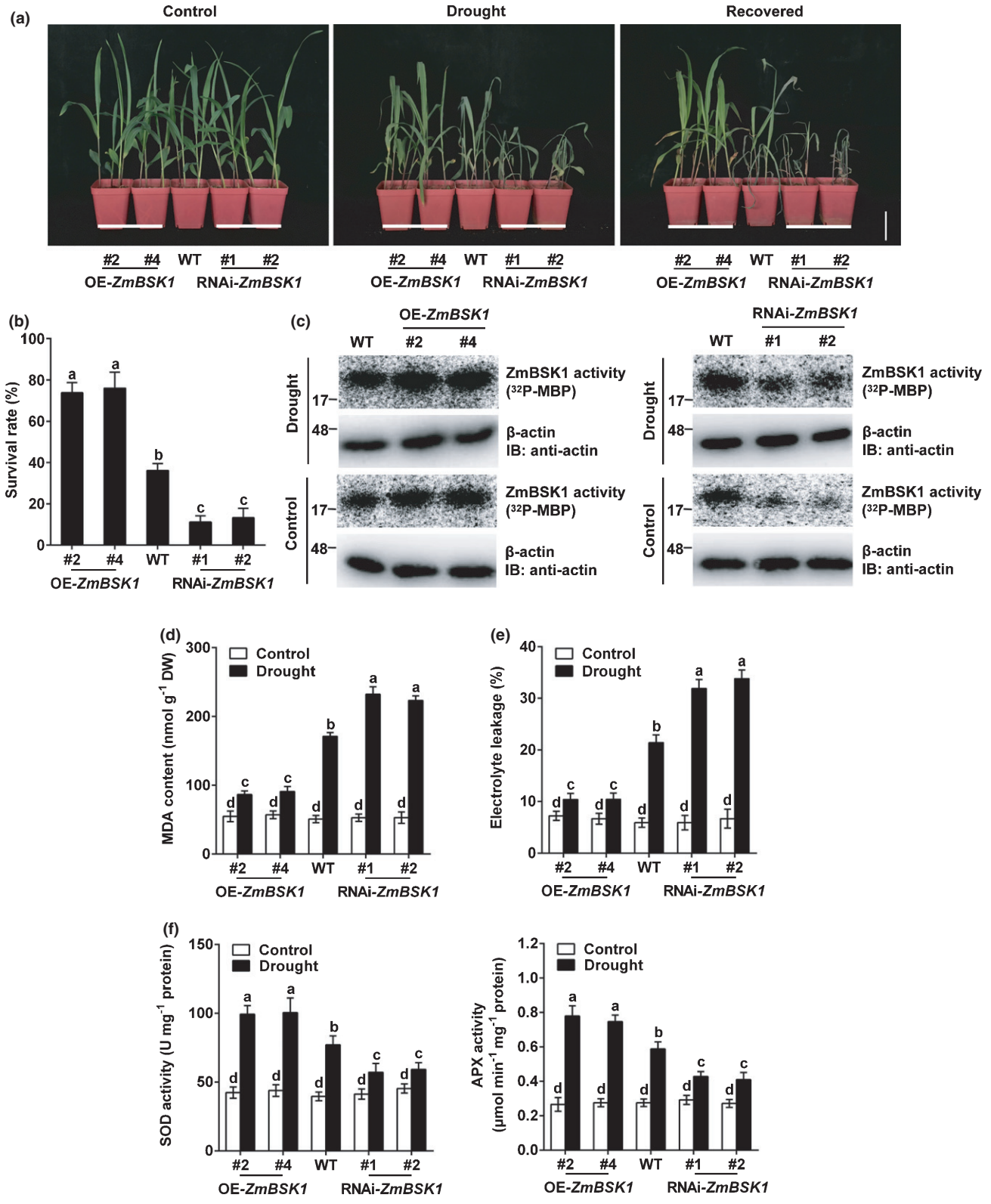

extracted the proteins from maize leaves and performed a Co-IP assay using specific anti-ZmBSK1 and anti-ZmCCaMK antibodies (Fig. S1; Methods S4, S5). Strong signals were detected when immunoblotting with specific anti-ZmBSK1 antibody (Fig. 1e). These observations suggest that ZmBSK1 physically interacts with ZmCCaMK.

To support the interaction between ZmBSK1 and ZmCCaMK, we transiently expressed ZmBSK1 or ZmCCaMK

© 2021 The Authors
New Phytologist © 2021 New Phytologist Foundation

14698137, 2021, 2, Downloaded from https://nph.onlinelibrary.wiley.com/doi/10.1111/nph.17403 by Zhejiang Agr & For University, Wiley Online Library on [17/10/2023]. See the Terms and Conditions (https://onlinelibrary.wiley.com/terms-and-conditions) on Wiley Online Library for rules of use; OA articles are governed by the applicable Creative Commons License

14698137, 2021, 2, Downloaded from https://nph.onlinelibrary.wiley.com/doi/10.1111/nph.17403 by Zhejiang Agr & For University, Wiley Online Library on [17/10/2023]. See the Terms and Conditions (https://onlinelibrary.wiley.com/terms-and-conditions) on Wiley Online Library for rules of use; OA articles are governed by the applicable Creative Commons License

Fig. 2 *Zea mays* brassinosteroid-signaling kinase 1 (ZmBSK1) positively regulates the tolerance of maize plants to drought stress. (a) Phenotype of overexpressing (OE)-*ZmBSK1*, RNA interference (RNAi)-*ZmBSK1* compared with wild-type (WT) plants under normal and drought stress conditions. Ten-day-old seedlings were subjected to progressive drought by withholding water for 6 d, and then rewatered and recovered for 3 d. Bar, 7 cm. All experiments were repeated at least three times with similar results. (b) Survival rate (%) of maize plants in (a) after recovery for 3 d. At least 30 seedlings of each line per replicate were used for survival rate analysis. Error bars represent SD ($n = 3$). Different letters indicate significant differences at $P < 0.05$ according to one-way ANOVA (Duncan's multiple range test). (c) The kinase activity of ZmBSK1 in OE-*ZmBSK1*, RNAi-*ZmBSK1* and WT plants exposed to drought stress. Ten-day-old seedlings were subjected to progressive drought by withholding water for 2 d. Seedlings treated with distilled water under the same conditions served as control. The kinase activity of ZmBSK1 was detected by immunoprecipitation kinase assay *in vitro*, and myelin basic protein (MBP) was used as substrate. β-actin was used as a loading control. The molecular weights are marked on the left. (d, e) The malondialdehyde (MDA) content (d) and the percentage leakage of electrolyte (e) in leaves of maize plants. Ten-day-old seedlings were subjected to progressive drought by withholding water for 2 d, and then the MDA content and the percentage leakage of electrolyte were measured. (f) Activities of superoxide dismutase (SOD) and ascorbate peroxidase (APX) in maize plants. Ten-day-old seedlings were subjected to progressive drought by withholding water for 2 d, and then the activities of SOD and APX were measured. Seedlings treated with distilled water under the same conditions served as controls. In (b) to (f), error bars represent SD ($n = 3$). Different letters indicate significant differences at $P < 0.05$ according to two-way ANOVA (Duncan's multiple range test).

with a YFP tag in maize mesophyll protoplasts. When ZmBSK1-YFP was transiently expressed in maize protoplasts, the YFP fluorescence signal was observed in the plasma membrane. When ZmCCaMK-YFP was transiently expressed in maize protoplasts, a strong YFP fluorescence signal was also observed in the plasma membrane (Fig. S2a,c; Methods S6). After expressing both ZmCCaMK-mCherry and ZmBSK1-YFP in maize protoplasts, colocalization of ZmCCaMK and ZmBSK1 in the plasma membrane was observed (Fig. S2b,d). Moreover, to assist in the observation in maize mesophyll protoplasts, we isolated the nucleus, the cytoplasm and the plasma membrane fractions from maize leaves and conducted immunoblot analysis (Methods S7). As shown in Fig. S2(e), the subcellular locations of ZmBSK1 and ZmCCaMK were consistent with those in Fig. S2a. Combined with the BiFC assay, we believe that ZmBSK1 interacts with ZmCCaMK in the plasma membrane.

ZmBSK1 positively affects drought tolerance

Zea mays calcium/calmodulin-dependentprotein kinase functions in drought stress responses (Ma *et al.*, 2012; Zhu *et al.*, 2016). Here, we investigated the effects of PEG-simulated drought stress (Duan *et al.*, 2017) on the subcellular locations of ZmBSK1 and ZmCCaMK, and found that PEG treatment did not affect the subcellular locations of them (Fig. S2e). Next, whether PEG treatment affects the interaction between ZmBSK1 and ZmCCaMK was studied. We treated maize seedlings with 10% PEG6000 for 90 min, extracted the proteins from maize leaves and performed a Co-IP assay using specific anti-ZmBSK1 and anti-ZmCCaMK antibodies. As shown in Fig. 1e, PEG treatment obviously enhanced the interaction between ZmBSK1 and ZmCCaMK, although the protein abundances of ZmBSK1 and ZmCCaMK were not affected.

Based on these results, we hypothesized that ZmBSK1 might have similar function to ZmCCaMK in response to drought. To test this hypothesis, we first investigated whether PEG-simulated drought stress activates ZmBSK1. The kinase activity of ZmBSK1 responses to PEG in maize was analyzed by immunoprecipitation kinase assays using specific anti-ZmBSK1 antibody. Myelin basic protein was used as an *in vitro* substrate and the kinase activity of ZmBSK1 was detected in the presence of Mn^{2+} (Fig. S3). As shown in Fig. S4, the activity of ZmBSK1 was activated as early as 15 min and maximized at 60 min after PEG treatment in maize leaves. The results suggest that drought can enhance the phosphorylation activity of ZmBSK1 in maize.

Next, to reveal the role of ZmBSK1 in maize under drought stress, we created transgene containing *ZmBSK1* coding sequence or RNA interference (RNAi) sequence and *Ubi* promoter, and stably introduced it into maize inbred line B73 (Fig. S5a). Two independent *ZmBSK1*-overexpressing lines (OE-*ZmBSK1*#2 and OE-*ZmBSK1*#4) were generated and the expression of ZmBSK1 at both the mRNA and protein levels were confirmed by quantitative RT-PCR and immunoblotting assays (Fig. S5b,c). Two independent *ZmBSK1*-knockdown lines (RNAi-*ZmBSK1*#1 and RNAi-*ZmBSK1*#2) were also generated. The gene expressions of a total of nine *ZmBSKs* were tested and only the *ZmBSK1* expression level was reduced by *c.* 75% in RNAi-*ZmBSK1* lines compared with the wild-type (Figs S5d, S6; Table S1). This shows that *ZmBSK1* expression is specially suppressed by RNAi. ZmBSK1 protein abundance was also obviously suppressed in RNAi-*ZmBSK1* lines compared with that in the wild-type (Fig. S5e).

Then, wild-type plants and OE-*ZmBSK1* and RNAi-*ZmBSK1* transgenic lines were subjected to drought stress. Under normal growth conditions, there was no significant difference in the growth of maize seedlings between wild-type and transgenic lines (Fig. 2a). However, under drought treatment, OE-*ZmBSK1* lines exhibited less severe wilting and chlorosis than wild-type plants, while RNAi-*ZmBSK1* lines exhibited more severe wilting and chlorosis (Fig. 2a). After recovery by rewatering, OE-*ZmBSK1* lines had higher survival rates, but RNAi-*ZmBSK1* lines had lower survival rates, than wild-type plants (Fig. 2b). Moreover, drought treatment obviously increased the activities of ZmBSK1 in wild-type and all transgenic lines (Fig. 2c). These results indicate that ZmBSK1 positively affects the tolerance to drought stress in maize.

Malondialdehyde content and electrolyte leakage are indicators of oxidative damage during stress treatment (Jiang & Zhang, 2002; Zhang *et al.*, 2011). Drought stress resulted in increases in the MDA content and percentage of electrolyte leakage compared with control conditions in wild-type plants, which were further aggravated in RNAi-*ZmBSK1* lines and were alleviated in OE-*ZmBSK1* lines (Fig. 2d,e). These results indicate that ZmBSK1 alleviates oxidative damage caused by drought stress in maize. Antioxidant defense system can scavenge drought-produced

© 2021 The Authors
New Phytologist © 2021 New Phytologist Foundation

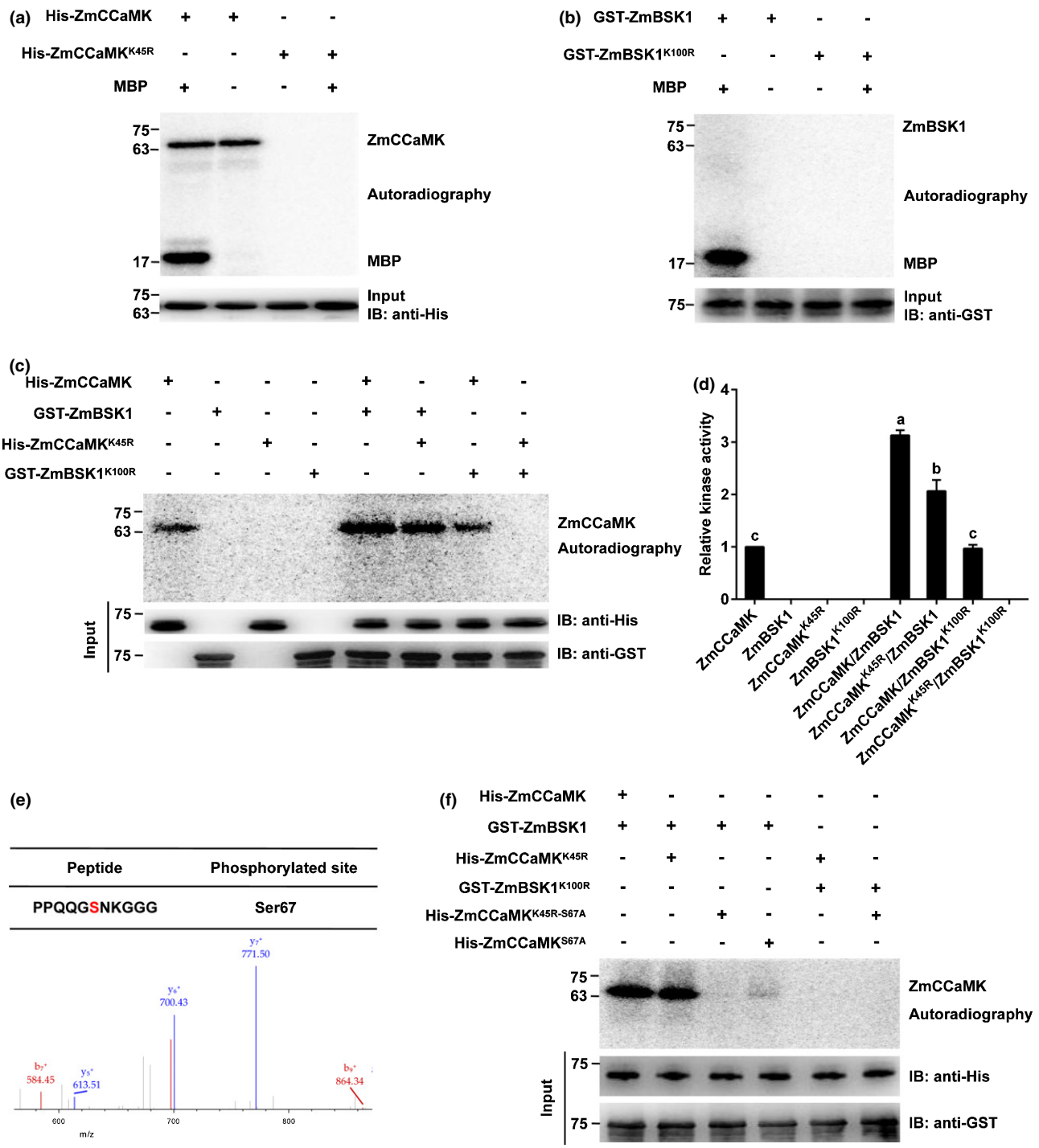

Fig. 3 *Zea mays* brassinosteroid-signaling kinase 1 (ZmBSK1) phosphorylates *Zea mays* calcium/calmodulin-dependent protein kinase (ZmCCaMK) *in vitro*. (a) ZmCCaMK^{K45R}, a kinase dead form of ZmCCaMK, absolutely blocks its autophosphorylation and phosphorylation activities. The kinase activities of purified His-ZmCCaMK and His-ZmCCaMK^{K45R} were detected by gel kinase assay *in vitro*, and myelin basic protein (MBP) was used as substrate. (b) ZmBSK1^{K100R}, a kinase dead form of ZmBSK1, absolutely blocks its kinase activity. The kinase activities of purified glutathione S-transferase (GST)-ZmBSK1 and GST-ZmBSK1^{K100R} were detected by gel kinase assay *in vitro*, and MBP was used as substrate. (c) ZmBSK1 phosphorylates ZmCCaMK. The phosphorylation of purified His-ZmCCaMK, His-ZmCCaMK^{K45R}, GST-ZmBSK1 and GST-ZmBSK1^{K100R} was detected by gel kinase assay *in vitro*. (d) Statistical analysis of ZmCCaMK kinase activity as shown in (c). The kinase activity of ZmCCaMK alone was set to 1. Error bars represent SD ($n = 3$). Different letters indicate significant differences at $P < 0.05$ according to one-way ANOVA (Duncan's multiple range test). (e) Phosphorylation analysis of the Ser67-phosphorylated peptides of ZmCCaMK by LC-MS/MS. The purified His-ZmCCaMK and GST-ZmBSK1 were incubated in kinase reaction buffer, and the phosphorylated ZmCCaMK was analyzed by LC-MS/MS. (f) Ser-67 is a crucial phosphorylation site of ZmCCaMK by ZmBSK1. The kinase activities of purified His-ZmCCaMK$^{K45R-S67A}$ and His-ZmCCaMK^{S67A} were detected by gel kinase assay *in vitro* in the presence of GST-ZmBSK1. ZmCCaMK and ZmBSK1 or their mutant proteins were analyzed by immunoblotting with anti-His or anti-GST antibody. The molecular weights are marked on the left. All experiments were repeated at least three times with similar results.

© 2021 The Authors
New Phytologist © 2021 New Phytologist Foundation

14698137, 2021, 2, Downloaded from https://nph.onlinelibrary.wiley.com/doi/10.1111/nph.17403 by Zhejiang Agr & For University, Wiley Online Library on [17/10/2023]. See the Terms and Conditions (https://onlinelibrary.wiley.com/terms-and-conditions) on Wiley Online Library for rules of use; OA articles are governed by the applicable Creative Commons License

14698137, 2021, 2, Downloaded from https://nph.onlinelibrary.wiley.com/doi/10.1111/nph.17403 by Zhejiang Agr & For University, Wiley Online Library on [17/10/2023]. See the Terms and Conditions (https://onlinelibrary.wiley.com/terms-and-conditions) on Wiley Online Library for rules of use; OA articles are governed by the applicable Creative Commons License

excess ROS to protect plants from oxidative damage (Jiang & Zhang, 2002; Cruz de Carvalho, 2008). Under drought stress, the activities of SOD and APX were increased in wild-type and transgenic lines. OE-*ZmBSK1* lines showed more increases in the activities of SOD and APX than did the wild-type, while RNAi-*ZmBSK1* lines showed fewer increases (Fig. 2f). No difference in SOD and APX activities was observed between wild-type plants and transgenic lines under the control conditions. These data indicate that ZmBSK1 positively regulates the antioxidant defense system to protect maize plants from oxidative damage under drought stress.

ZmBSK1 phosphorylates ZmCCaMK *in vitro*

Both BSK1 and CCaMK have kinase activity and can phosphorylate their substrates to function in diverse biological processes (Kim *et al.*, 2009; Zhang *et al.*, 2016; Zhu *et al.*, 2016). To investigate what is the phosphorylation substrate between ZmCCaMK and ZmBSK1, we attempted to generate the kinase-dead forms of ZmCCaMK and ZmBSK1. The conserved ATP binding sites Lys-45 (K45) in ZmCCaMK and Lys-100 (K100) in ZmBSK1 (Fig. S7) were mutated to Arg (R) to generate ZmCCaMK and ZmBSK1 mutant forms (ZmCCaMK^{K45R} and ZmBSK1^{K100R}) (Methods S8) (Yano *et al.*, 2008; Bayer *et al.*, 2009; Miller *et al.*, 2013; Shi *et al.*, 2013; Pimprikar *et al.*, 2016; Ren *et al.*, 2019). To determine whether ZmCCaMK^{K45R} and ZmBSK1^{K100R} are kinase-dead, an *in vitro* kinase assay was performed using MBP as substrate. As shown in Fig. 3(a), His-ZmCCaMK exhibited both strong autophosphorylation and transphosphorylation activities, whereas His-ZmCCaMK^{K45R} showed neither autophosphorylation nor transphosphorylation activity. GST-ZmBSK1 and GST-ZmBSK1^{K100R} did not exhibit autophosphorylation activity, and MBP was only phosphorylated by GST-ZmBSK1 but not GST-ZmBSK1^{K100R} (Fig. 3b). These results indicate that His-ZmCCaMK^{K45R} and GST-ZmBSK1^{K100R} do not have kinase activity, which are kinase-dead forms of ZmCCaMK and ZmBSK1, respectively. Next, the phosphorylation between ZmCCaMK and ZmBSK1 was studied. Our results showed that the phosphorylation of His-ZmCCaMK was largely enhanced by GST-ZmBSK1 compared with His-ZmCCaMK alone or by GST-ZmBSK1^{K100R}, suggesting that His-ZmCCaMK and His-ZmCCaMK^{K45R} could be phosphorylated by GST-ZmBSK1. However, there was no phosphorylation of GST-ZmBSK1 or GST-ZmBSK1^{K100R} by His-ZmCCaMK (Fig. 3c,d). These results indicate that ZmBSK1 can phosphorylate ZmCCaMK *in vitro*.

To determine the phosphorylation site(s) of ZmCCaMK by ZmBSK1, His-ZmCCaMK protein was incubated with or without GST-ZmBSK1 protein in kinase reaction buffer and was then analyzed by LC-MS/MS. The three independent experiment results showed that some potential autophosphorylation sites of ZmCCaMK were identified in the absence of ZmBSK1 (Table S2), while a novel phosphorylation site Ser-67 (S67, -PPQQGpSNKGGG-) was detected in ZmCCaMK in the presence of ZmBSK1 (Fig. 3e; Table S3). To confirm Ser-67 is the phosphorylation site of ZmCCaMK by ZmBSK1, we generated His-ZmCCaMK^{S67A} and His-ZmCCaMK$^{K45R-S67A}$ nonphosphorylation mutant forms by replacement of Ser-67 with Ala. And the results showed that the phosphorylation of ZmCCaMK by ZmBSK1 was dramatically abolished in ZmCCaMK^{S67A} and ZmCCaMK$^{K45R-S67A}$ mutants (Fig. 3f). These results indicate that Ser-67 is a crucial site for ZmCCaMK phosphorylation by ZmBSK1 *in vitro*.

ZmBSK1 phosphorylates ZmCCaMK at Ser-67 *in vivo* and drought enhances this phosphorylation

To determine the phosphorylation of ZmCCaMK by ZmBSK1 in maize, we extracted total proteins from maize leaves and performed an immunoblotting assay using specific anti-pSer67-ZmCCaMK antibody (Fig. S8). As shown in Fig. 4(a), the phosphorylation of Ser-67 in ZmCCaMK was clearly observed, indicating that ZmCCaMK is phosphorylated at Ser-67 in maize. Furthermore, the activity of ZmCCaMK and the phosphorylation of Ser-67 of ZmCCaMK in OE-*ZmBSK1* and RNAi-*ZmBSK1* transgenic lines were tested. The results showed that the kinase activity of ZmCCaMK or the phosphorylation of Ser-67 of ZmCCaMK in OE-*ZmBSK1* lines was stronger than that in wild-type plants, while that in RNAi-*ZmBSK1* lines was really weaker (Fig. 4e–h). These results indicate that ZmBSK1 phosphorylates ZmCCaMK at Ser-67 *in vivo*.

To explore the effect of drought on the phosphorylation of ZmCCaMK by ZmBSK1 and the kinase activity of ZmCCaMK, maize plants were treated with 10% PEG6000 for various lengths of time. The results showed that the phosphorylation of Ser-67 of ZmCCaMK and the kinase activity of ZmCCaMK had a more significant enhancement in wild-type plants and OE-*ZmBSK1* lines than that in RNAi-*ZmBSK1* lines after PEG treatment (Fig. 4). Taken together, these results indicate that drought enhances the phosphorylation of Ser-67 of ZmCCaMK and the kinase activity of ZmCCaMK in a ZmBSK1-dependent manner in maize.

Ser-67 phosphorylation in ZmCCaMK affects its autophosphorylation activity and transphosphorylation activity

The kinase activity of CCaMK is regulated by autophosphorylation and transphosphorylation (Sathyanarayanan *et al.*, 2000). To understand the role of phosphorylation of Ser-67 in the activation of ZmCCaMK, Ser-67 of ZmCCaMK was also mutated to Asp (ZmCCaMK^{S67D}) to generate a phosphomimetic mutant. Then we analyzed the autophosphorylation and transphosphorylation activities of ZmCCaMK, ZmCCaMK^{S67A} and ZmCCaMK^{S67D}. In the absence of Ca^{2+}, ZmCCaMK, ZmCCaMK^{S67A} and ZmCCaMK^{S67D} all had very weak autophosphorylation and transphosphorylation activities (Fig. 5). In the presence of Ca^{2+}, replacement of Ser-67 with Ala dramatically weakened the autophosphorylation activity of ZmCCaMK, while S67D mutation significantly enhanced its autophosphorylation activity (Fig. 5a,c). A similar pattern was also observed in transphosphorylation activity of ZmCCaMK in the presence of

© 2021 The Authors
New Phytologist © 2021 New Phytologist Foundation

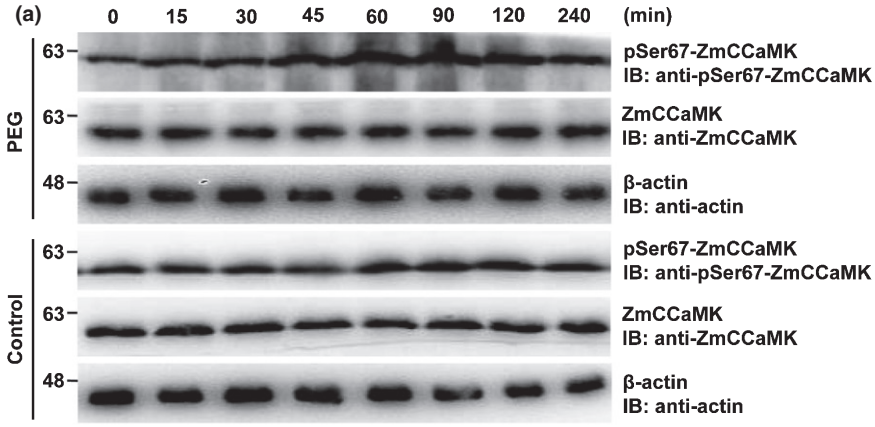

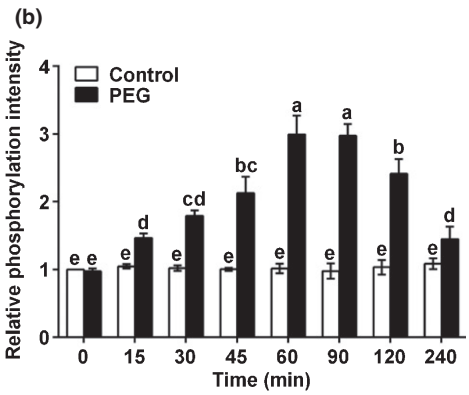

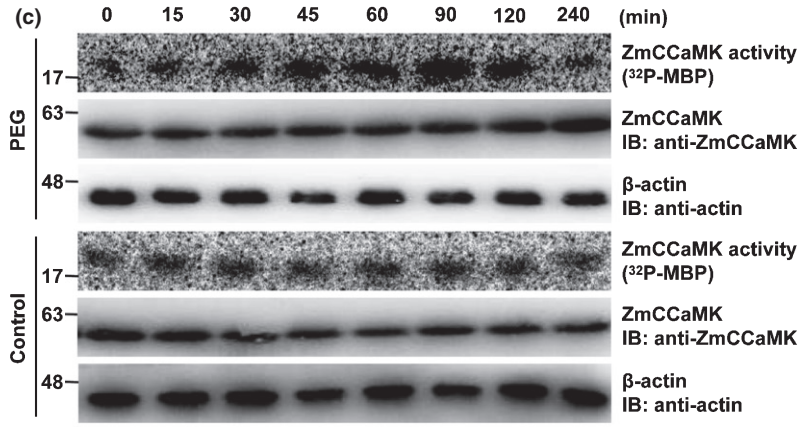

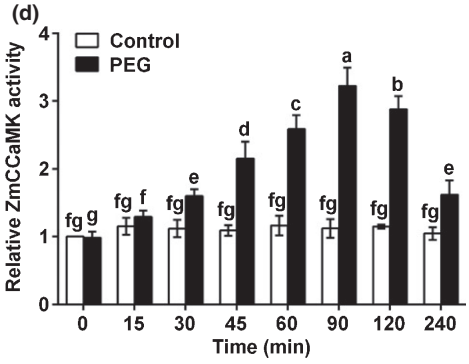

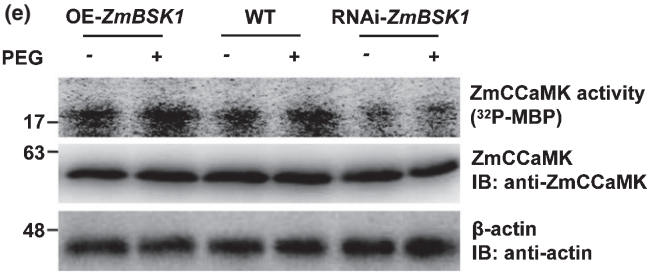

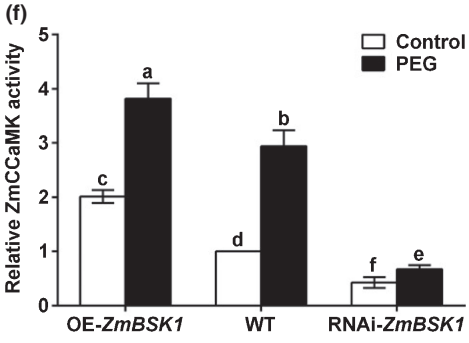

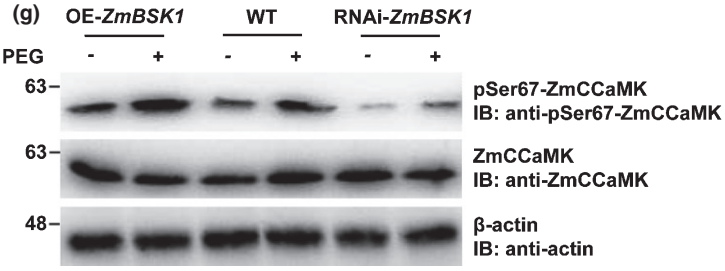

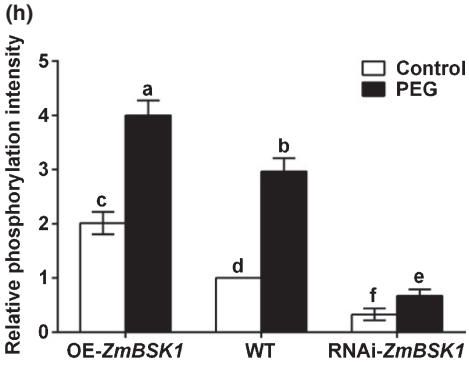

Ca^{2+}/CaM. His-ZmCCaMK^{S67A} exhibited the weakest transphosphorylation activity, while His-ZmCCaMK^{S67D} showed the strongest activity (Fig. 5b,d). These results suggest that Ser-67 phosphorylation affects the autophosphorylation and transphosphorylation activities of ZmCCaMK.

Ser-67 phosphorylation contributes to the role of ZmCCaMK in drought stress tolerance in maize

Next, we wondered if the Ser-67 phosphorylation of ZmCCaMK would affect its function in drought tolerance. To test this, two

© 2021 The Authors
New Phytologist © 2021 New Phytologist Foundation

14698137, 2021, 2, Downloaded from https://nph.onlinelibrary.wiley.com/doi/10.1111/nph.17403 by Zhejiang Agr & For University, Wiley Online Library on [17/10/2023]. See the Terms and Conditions (https://onlinelibrary.wiley.com/terms-and-conditions) on Wiley Online Library for rules of use; OA articles are governed by the applicable Creative Commons License

14698137, 2021, 2, Downloaded from https://nph.onlinelibrary.wiley.com/doi/10.1111/nph.17403 by Zhejiang Agr & For University, Wiley Online Library on [17/10/2023]. See the Terms and Conditions (https://onlinelibrary.wiley.com/terms-and-conditions) on Wiley Online Library for rules of use; OA articles are governed by the applicable Creative Commons License

Fig. 4 Polyethylene glycol (PEG) induces the phosphorylation of Ser67-*Zea mays* calcium/calmodulin-dependent protein kinase (ZmCCaMK) and the kinase activity of ZmCCaMK in a *Zea mays* brassinosteroid-signaling kinase 1 (ZmBSK1)-dependent manner. (a) Phosphorylation of Ser67-ZmCCaMK (pSer67-ZmCCaMK) in maize plants exposed to PEG treatment. The maize seedlings were treated with or without 10% PEG6000 for various lengths of time, as indicated. Total proteins extracted from the leaves were used for immunoblotting with anti-phosphorylated Ser67 (pSer67)-ZmCCaMK antibody. (b) Statistical analysis of pSer67-ZmCCaMK as shown in (a). The intensity of pSer67-ZmCCaMK in the control at 0 min was set to 1. (c) Kinase activity of ZmCCaMK in maize plants exposed to PEG treatment. The maize seedlings were treated with or without 10% PEG6000 for various lengths of time, as indicated. The kinase activity of ZmCCaMK was detected by immunoprecipitation kinase assay *in vitro*, and myelin basic protein (MBP) was used as substrate. (d) Statistical analysis of the kinase activity of ZmCCaMK as shown in (c). The kinase activity of ZmCCaMK in the control at 0 min was set to 1. (e) The kinase activity of ZmCCaMK in overexpressing (OE)-*ZmBSK1*#2, RNAi interference (RNAi)-*ZmBSK1*#1 and wild-type (WT) plants. Ten-day-old seedlings were treated with or without 10% PEG6000 for 90 min. The kinase activity of ZmCCaMK was detected by immunoprecipitation kinase assay *in vitro*, and MBP was used as substrate. (f) Statistical analysis of the kinase activity of ZmCCaMK as shown in (e). The kinase activity of ZmCCaMK in the control of WT was set to 1. (g) Phosphorylation of Ser67-ZmCCaMK (pSer67-ZmCCaMK) in OE-*ZmBSK1*#2, RNAi-*ZmBSK1*#1 and WT plants. Ten-day-old seedlings were treated with or without 10% PEG6000 for 90 min. Total proteins extracted from the leaves were used for immunoblotting with anti-pSer67-ZmCCaMK antibody. (h) Statistical analysis of pSer67-ZmCCaMK as shown in (g). The intensity of pSer67-ZmCCaMK in the control of WT was set to 1. In (a), (c), (e) and (g), the protein abundance of ZmCCaMK was analyzed by immunoblotting with anti-ZmCCaMK antibody and β-actin was used as a loading control. The molecular weights are marked on the left. All experiments were repeated at least three times with similar results. In (b), (d), (f) and (h), error bars represent SD ($n = 3$). Different letters indicate significant differences at $P < 0.05$ according to two-way ANOVA (Duncan's multiple range test).

independent *ZmCCaMK*^{S67A}-overexpressing lines, two independent *ZmCCaMK*^{S67D}-overexpressing lines and two independent *ZmCCaMK*-overexpressing lines were generated and confirmed by qRT-PCR and immunoblotting assay using specific anti-ZmCCaMK antibody (Fig. S4f,g). Then these transgenic lines and wild-type plants were treated with drought and used to analyze the role of Ser-67 phosphorylation in ZmCCaMK. When compared with *ZmCCaMK*-overexpressing and *ZmCCaMK*^{S67A}-overexpressing plants, *ZmCCaMK*^{S67D}-overexpressing plants showed less severe wilting and chlorosis after drought treatment (Fig. 6a). After recovery by rewatering, the survival rate of *ZmCCaMK*^{S67D}-overexpressing lines was higher than that of *ZmCCaMK*-overexpressing lines, while that of *ZmCCaMK*^{S67A}-overexpressing lines was lower (Fig. 6b). A similar pattern was also observed in the activities of SOD and APX (Fig. 6e). Moreover, the MDA content (Fig. 6c) and the percentage of electrolyte leakage (Fig. 6d) were lower in *ZmCCaMK*^{S67D}-overexpressing plants than those in *ZmCCaMK*-overexpressing plants, and higher in *ZmCCaMK*^{S67A}-overexpressing plants after exposure to drought treatment. No significant difference was observed under well-watered conditions. These results indicate that phosphorylation of Ser-67 in ZmCCaMK plays a positive role in drought tolerance of maize plants.

Ser-67 phosphorylation in ZmCCaMK promotes its binding to Ca^{2+} and CaM

The autophosphorylation activity of CCaMK was regulated by the binding of Ca^{2+} (Miller *et al.*, 2013). To study whether phosphorylation of Ser-67 in ZmCCaMK affects Ca^{2+} binding to ZmCCaMK, a gel shift assay (Vallone *et al.*, 2016) was performed. The results showed that ZmCCaMK, ZmCCaMK^{S67A} and ZmCCaMK^{S67D} had no obvious migration in the absence of Ca^{2+}. However, in the presence of Ca^{2+}, ZmCCaMK^{S67D} displayed an especially faster mobility than ZmCCaMK, while ZmCCaMK^{S67A} showed a slower electrophoretic mobility (Fig. 7a). Similarly, $^{45}Ca^{2+}$ overlay assay (Masumi *et al.*, 1998) also showed that Ca^{2+} binding to ZmCCaMK was enhanced in ZmCCaMK^{S67D} but was sharply blocked in ZmCCaMK^{S67A} (Fig. 7b). These results indicate that phosphorylation of Ser-67 in ZmCCaMK promotes the binding of Ca^{2+} to ZmCCaMK.

Besides Ca^{2+}, CaM also affected the transphosphorylation activity of CCaMK (Sathyanarayanan *et al.*, 2000; Miller *et al.*, 2013). We detected the CaM-binding capacity of ZmCCaMK using a CaM-binding assay (Arazi *et al.*, 1995). The purified His-ZmCCaMK, His-ZmCCaMK^{S67D} and His-ZmCCaMK^{S67A} were separated by SDS-PAGE, blotted onto polyvinylidene difluoride membrane, and incubated with purified GST-ZmCaM1. The overlay signal was then detected using anti-GST antibody. As shown in Fig. 7(c), in the presence of Ca^{2+}, ZmCCaMK^{S67D} exhibited stronger binding ability to ZmCaM1 than ZmCCaMK, while ZmCCaMK^{S67A} showed weaker binding affinity. In the absence of Ca^{2+}, none of ZmCCaMK, ZmCCaMK^{S67A} and ZmCCaMK^{S67D} could bind to ZmCaM1. To confirm the effects of phosphorylation of Ser-67 on the binding ability of ZmCCaMK to ZmCaM1, a Co-IP assay was subsequently performed. Similarly, ZmCCaMK bound to ZmCaM1, which was enhanced by the phosphomimetic mutation (ZmCCaMK^{S67D}) and weakened by the nonphosphorylatable mutation (ZmCCaMK^{S67A}) (Fig. 7d). These results indicate that phosphorylation of ZmCCaMK at Ser-67 promotes its binding to Ca^{2+} and CaM.

Discussion

Brassinosteroid-signaling kinase proteins play a very important role in BR signaling transduction, and BSK family proteins are discovered in many species (Tang *et al.*, 2008; Zhang *et al.*, 2016; Wang *et al.*, 2017; Li *et al.*, 2019). BSK1 and BSK2 in *Arabidopsis* contribute to YDA activation in the early embryo (Neu *et al.*, 2019). OsBSK1-2 does not affect plant architecture or response to BR, while OsBSK3 positively regulates BR signaling in *Arabidopsis* and rice (Zhang *et al.*, 2016; Wang *et al.*, 2017; Ren *et al.*, 2019). Besides that, BSKs also function in stress responses. BSK1 functions as a major regulator in plant immunity and physically associates with FLS2 (Shi *et al.*, 2013; Wang

© 2021 The Authors
New Phytologist © 2021 New Phytologist Foundation

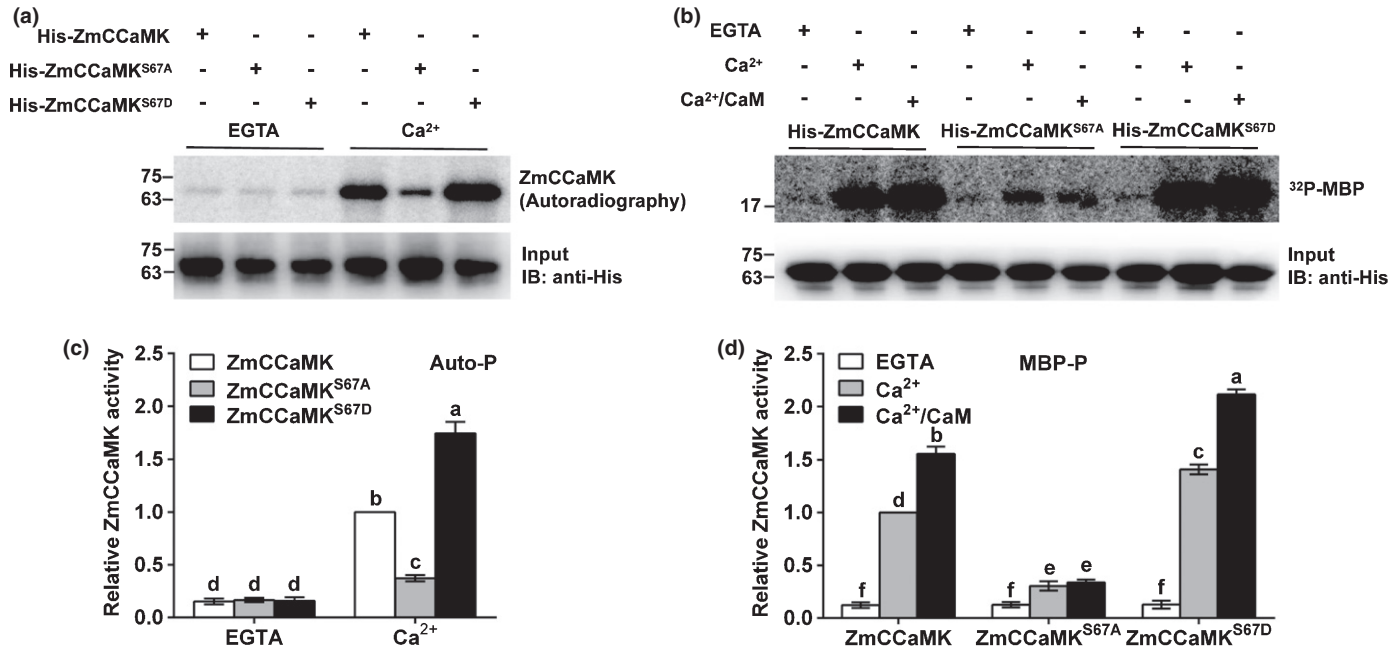

Fig. 5 The phosphorylation of Ser67-*Zea mays* calcium/calmodulin-dependent protein kinase (ZmCCaMK) positively regulates its kinase activity. (a) Phosphorylation of Ser67-ZmCCaMK enhances its autophosphorylation activity. The autophosphorylation activities of purified His-ZmCCaMK, His-ZmCCaMK^{S67A} and His-ZmCCaMK^{S67D} were detected by gel kinase assay *in vitro* in the presence of 5 mM EGTA or 1 mM $CaCl_2$. His-ZmCCaMK and its mutant proteins were analyzed by immunoblotting with anti-His antibody. (b) Phosphorylation of Ser67-ZmCCaMK enhances its transphosphorylation activity. The phosphorylation activities of purified His-ZmCCaMK, His-ZmCCaMK^{S67A} and His-ZmCCaMK^{S67D} were detected by gel kinase assay *in vitro* in the presence of 5 mM EGTA, 1 mM $CaCl_2$ or 1 μM calmodulin (CaM) (containing 1 mM $CaCl_2$). Myelin basic protein (MBP) was used as substrate. His-ZmCCaMK and its mutant proteins were analyzed by immunoblotting with anti-His antibody. (c) Statistical analysis of autophosphorylation activity as shown in (a). The autophosphorylation activity of His-ZmCCaMK in the presence of 1 mM $CaCl_2$ was set to 1. (d) Statistical analysis of phosphorylation activity as shown in (b). The transphosphorylation activity of His-ZmCCaMK in the presence of 1 mM $CaCl_2$ was set to 1. The molecular weights are marked on the left. All experiments were repeated at least three times with similar results. In (c) and (d), error bars represent SD ($n = 3$). Different letters indicate significant differences at $P < 0.05$ according to two-way ANOVA (Duncan's multiple range test).

et al., 2017; Yan *et al.*, 2018). BSK5 plays a role in pattern-triggered immunity and responds to salt, drought, cold, BR and ABA at the transcriptional level (Li *et al.*, 2012; Majhi *et al.*, 2019). However, the function of BSKs is still quite limited. In this study, we revealed an important role of ZmBSK1, an ortholog of AtBSK1 in maize (Fig. S9; Methods S9, S10), in drought stress response. ZmBSK1 increased the activities of antioxidant defense enzymes, protected plants from oxidative damage, and positively improved the tolerance to drought in maize (Fig. 2). BSK5 loss-of-function mutant, *bsk5*, shows more tolerance to water shortage (Li *et al.*, 2012). ZmBSK1 exhibits the opposite role to BSK5 in drought stress. The different responses among the members of the BSK family are also observed in other studies. Among 10 *bsk* mutants (*bsk1*, *2*, *3*, *4*, *5*, *6*, *8*, *10*, *11*, and *12*), only the *bsk3-1* mutant, different from other mutants, does not exhibit obvious growth phenotypes and BR resistance (Ren *et al.*, 2019). Similarly, BSK3, BSK4, BSK7 and BSK8 belong to the same clade of the BSK family phylogenetic tree and appear to functionally overlap in regulating BR signaling, while BSK1 shows distinct functional characteristics (Sreeramulu *et al.*, 2013). Genome-wide transcriptome analysis reveals different transcriptional responses of BSKs to drought stress in two Tibetan annual wild barley genotypes XZ5 (drought-tolerant) and XZ54 (drought-sensitive) (Chen *et al.*, 2019). *BSK1* is upregulated in XZ5 but downregulated in XZ54 under drought stress. By contrast, *BSK2* is downregulated in XZ5 but upregulated in XZ54, and *BSK5* is downregulated in both XZ5 and XZ54. Moreover, each of the BSKs displays a unique expression pattern at various development stages (Sreeramulu *et al.*, 2013). These findings suggest the diversity of BSK function. BSKs may generate different signaling outputs and function in different development or stress processes. Discovering the detailed BSK function mechanisms requires the identification of different components downstream of BSKs family members.

Brassinosteroid-signaling kinases interact with BRI1, BSU1, BIN2 and the members of their family (Tang *et al.*, 2008; Sreeramulu *et al.*, 2013; Ren *et al.*, 2019). Here, we identified that ZmCCaMK is a novel interaction protein of ZmBSK1. Our results showed that ZmBSK1 directly interacted with ZmCCaMK *in vitro* and *in vivo* (Fig. 1). BSK1 has kinase activity. BSK1 phosphorylates its target BSU1 to transduce BR signal to downstream targets (Kim *et al.*, 2009) and phosphorylates MAPKKK5 to regulate plant immunity (Yan *et al.*, 2018). Meanwhile, CCaMK also has kinase activity and CIP73, IPD3/CYCLOPS and NAC84 are identified as its substrates (Yano *et al.*, 2008; Kang *et al.*, 2011; Zhu *et al.*, 2016). Both ZmBSK1

© 2021 The Authors
New Phytologist © 2021 New Phytologist Foundation

14698137, 2021, 2, Downloaded from https://nph.onlinelibrary.wiley.com/doi/10.1111/nph.17403 by Zhejiang Agr & For University, Wiley Online Library on [17/10/2023]. See the Terms and Conditions (https://onlinelibrary.wiley.com/terms-and-conditions) on Wiley Online Library for rules of use; OA articles are governed by the applicable Creative Commons License

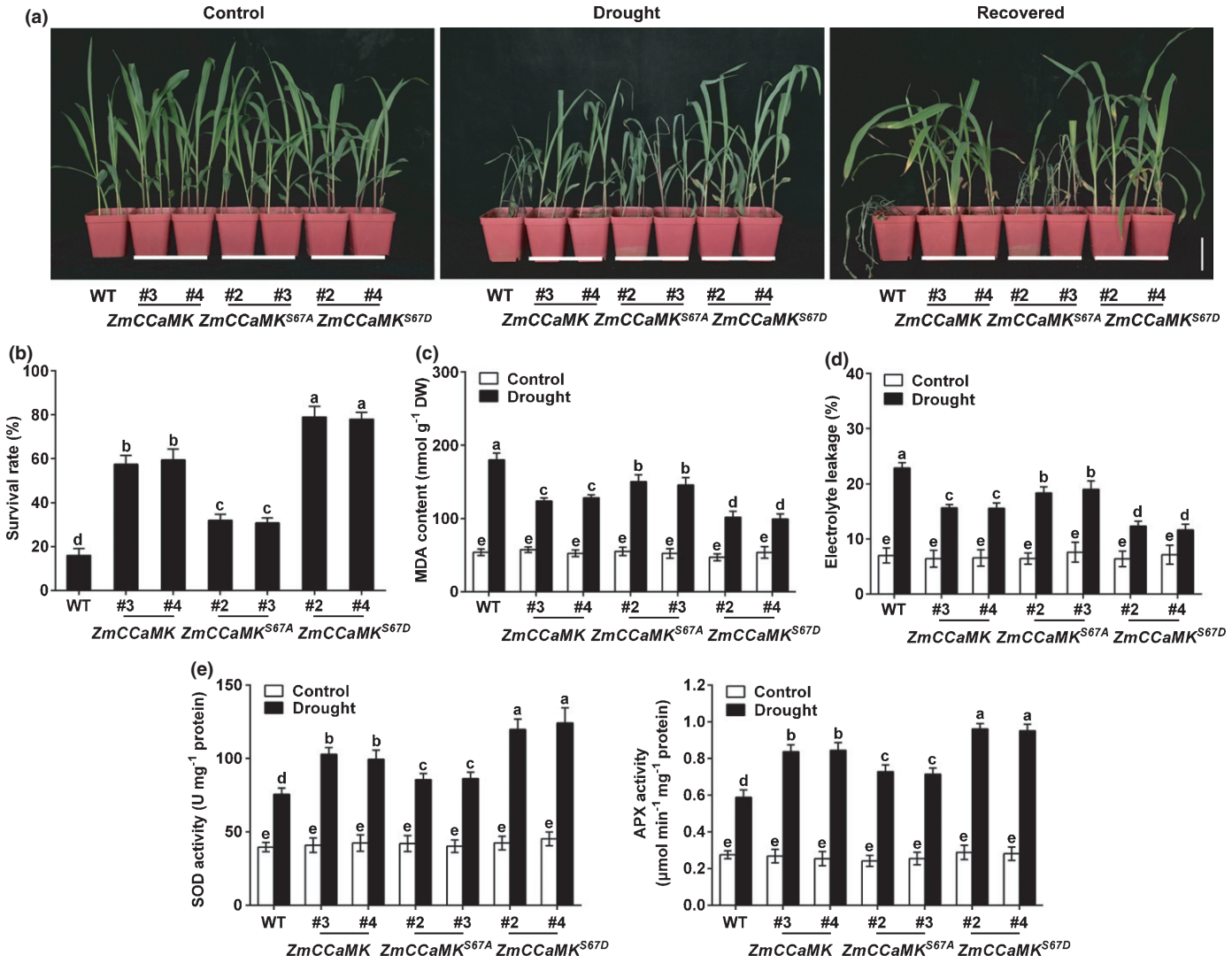

Fig. 6 The phosphorylation of Ser67-*Zea mays* calcium/calmodulin-dependent protein kinase (ZmCCaMK) positively regulates the tolerance of maize plants to drought stress. (a) Phenotype of overexpressing (OE)-*ZmCCaMK*, OE-*ZmCCaMK*^{S67A}, OE-*ZmCCaMK*^{S67D} compared with wild-type (WT) plants under normal and drought stress conditions. Ten-day-old seedlings were subjected to progressive drought by withholding water for 8 d, and then rewatered and allowed to recovered for 3 d. Bar, 7 cm. All experiments were repeated at least three times with similar results. (b) The survival rate (%) of maize plants in (a) after recovered for 3 d. At least 30 seedlings of each line per replicate were used for survival rate analysis. Error bars represent SD ($n = 3$). Different letters indicate significant differences at $P < 0.05$ according to one-way ANOVA (Duncan's multiple range test). (c, d) The malondialdehyde (MDA) content (c) and percentage leakage of electrolyte (d) in leaves of maize plants. Ten-day-old seedlings were subjected to progressive drought by withholding water for 2 d, and then the MDA content and the percentage leakage of electrolyte were measured. (e) Activities of superoxide dismutase (SOD) and ascorbate peroxidase (APX) in maize plants. Ten-day-old seedlings were subjected to progressive drought by withholding water for 2 d, and then the activities of SOD and APX were measured. Seedlings treated with distilled water under the same conditions served as control. In (c–e), error bars represent SD ($n = 3$). Different letters indicate significant differences at $P < 0.05$ according to two-way ANOVA (Duncan's multiple range test).

and ZmCCaMK are kinase proteins, and therefore it is worthy to clarify the phosphorylation relationship between ZmBSK1 and ZmCCaMK. Interestingly, we identified ZmCCaMK as a downstream phosphorylation substrate of ZmBSK1 (Figs 1, 3, 4). ZmBSK1 could directly phosphorylate ZmCCaMK, but ZmCCaMK could not phosphorylate ZmBSK1, and Ser-67 was a crucial phosphorylation site of ZmCCaMK by ZmBSK1.

ZmBSK1 localized in the plasma membrane and the N-terminal myristoylation site (Gly-2) was responsible for its subcellular localization (Fig. S10) (Thompson Jr & Okuyama, 2000). Membrane localization is essential to the function of BSKs. AtBSK1^{G2A} mutant form is unable to complement the *bsk1-1* phenotype (Shi *et al.*, 2013) and overexpression of *OsBSK3*^{G2A} in *bri1-5* plants is also unable to rescue the semi-dwarf phenotype of the mutants (Zhang *et al.*, 2016). ZmCCaMK physically interacts with ZmBSK1 in the plasma membrane, and has overlapping function in plant response to drought stress (Figs 1, 2, 6, S2) (Ma *et al.*, 2012; Zhu *et al.*, 2016), suggesting that ZmCCaMK and ZmBSK1 function in drought stress together. Drought significantly enhanced the interaction between ZmBSK1 and ZmCCaMK (Fig. 1e). Accompanied by the increasing kinase activity of ZmCCaMK, the

© 2021 The Authors
New Phytologist © 2021 New Phytologist Foundation

14698137, 2021, 2, Downloaded from https://nph.onlinelibrary.wiley.com/doi/10.1111/nph.17403 by Zhejiang Agr & For University, Wiley Online Library on [17/10/2023]. See the Terms and Conditions (https://onlinelibrary.wiley.com/terms-and-conditions) on Wiley Online Library for rules of use; OA articles are governed by the applicable Creative Commons License

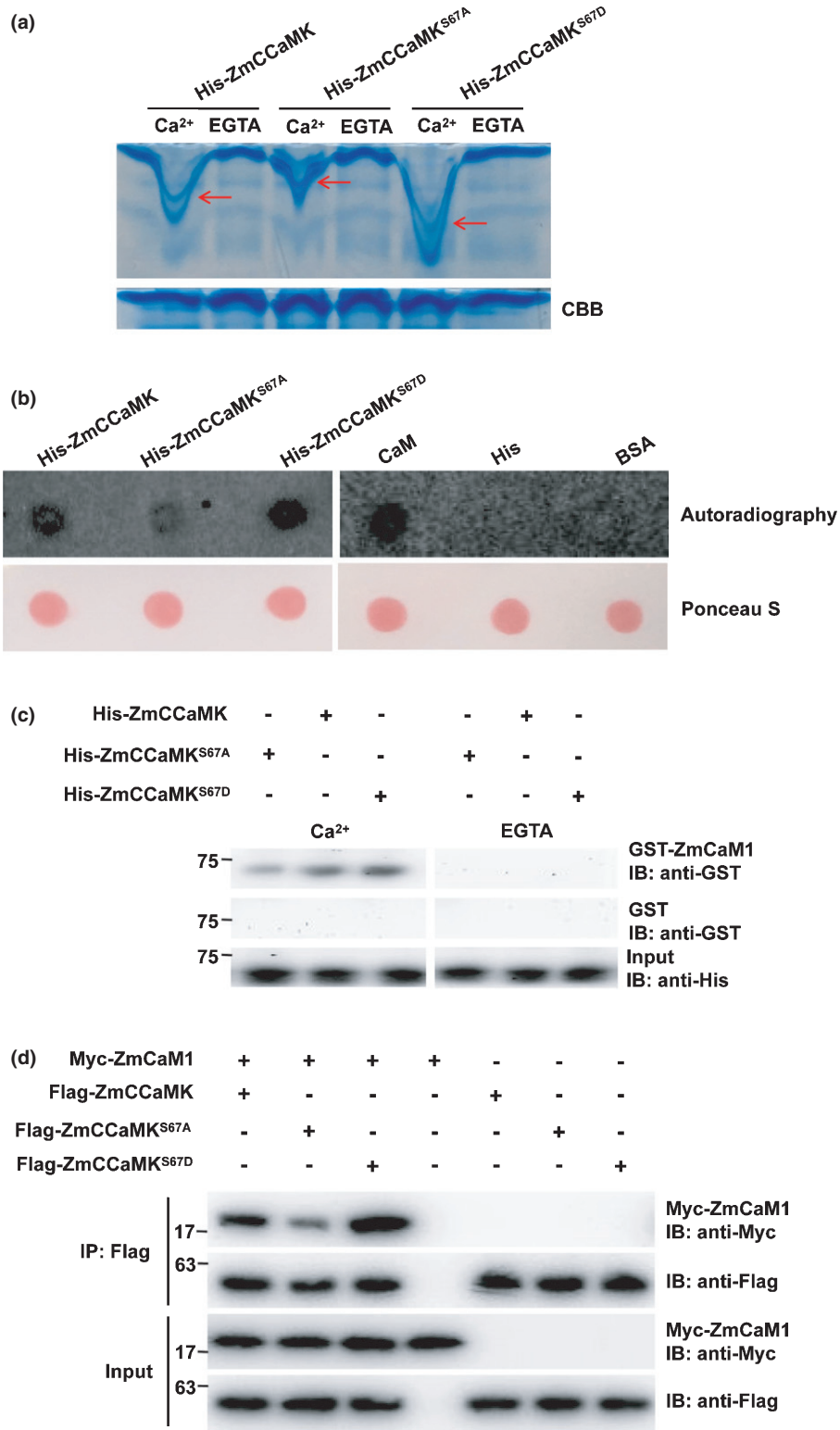

Fig. 7 The phosphorylation of Ser-67 in *Zea mays* calcium/calmodulin-dependent protein kinase (ZmCCaMK) modulates its ability to bind Ca^{2+} and calmodulin (CaM). (a) Gel shift assay of Ca^{2+} binding to His-ZmCCaMK and its mutant proteins. The purified His-ZmCCaMK, His-ZmCCaMK^{S67A} and His-ZmCCaMK^{S67D} were incubated with 5 mM $CaCl_2$ or 10 mM EGTA for 15 min and then separated by 12% native polyacrylamide gel electrophoresis (PAGE) (upper panel). The red arrows show the migrated location of these proteins. Coomassie brilliant blue (CBB) staining was used as a loading control (lower panel). (b) $^{45}Ca^{2+}$ overlay assay of Ca^{2+} binding to His-ZmCCaMK and its mutant proteins. The purified His-ZmCCaMK, His-ZmCCaMK^{S67A} and His-ZmCCaMK^{S67D} were spotted on a nitrocellulose (NC) membrane and incubated with 1 μCi $^{45}Ca^{2+}$. Calmodulin, His and bovine serum albumin (BSA) were used as positive, blank and negative control, respectively. $^{45}Ca^{2+}$ signals were detected by autoradiography (upper panel). Ponceau S staining was used as a loading control (lower panel). (c) Calmodulin-binding assay of *Z. mays* calmodulin 1 (ZmCaM1) binding to His-ZmCCaMK and its mutant proteins. The purified His-ZmCCaMK, His-ZmCCaMK^{S67A} and His-ZmCCaMK^{S67D} were separated and transferred to a polyvinylidene fluoride (PVDF) membrane, and were probed with purified glutathione S-transferase (GST)-ZmCaM1 in the presence of 5 mM $CaCl_2$ or 10 mM EGTA, and then the binding ZmCaM1 was detected by immunoblotting with anti-GST antibody. Glutathione S-transferase was used as a negative control. His-ZmCCaMK and its mutant proteins were analyzed by immunoblotting with anti-His antibody. (d) Coimmunoprecipitation (Co-IP) assay of ZmCaM1 binding to His-ZmCCaMK and its mutant proteins. Fusion constructs *35S:Myc-ZmCaM1* and *35S:Flag-ZmCCaMK* or its mutants were transiently expressed in tobacco (*Nicotiana benthamiana*) leaves simultaneously or separately. Total protein extracts were immunoprecipitated with anti-Flag antibody. ZmCaM1 and ZmCCaMK or its mutant proteins were detected by immunoblotting with anti-Myc and anti-Flag antibodies, respectively. The molecular weights are marked on the left. All experiments were repeated at least three times with similar results.

phosphorylation at Ser-67 of ZmCCaMK kept growing in response to drought stress (Figs 3, 4). More importantly, the increases in both Ser-67 phosphorylation and the kinase activity of ZmCCaMK were ZmBSK1-dependent in maize (Fig. 4e–h). Furthermore, genetic analysis revealed that Ser-67 phosphorylation of ZmCCaMK by ZmBSK1 played a critical role in regulating drought tolerance in maize (Fig. 6). Together, these results confirm that ZmBSK1 phosphorylates ZmCCaMK at Ser-67 in maize drought tolerance.

The revealed activation mechanisms of CCaMKs show that Ca^{2+} binding to the EF-hands of CCaMK promotes its autophosphorylation, and enhances the binding of Ca^{2+}/CaM,

© 2021 The Authors
New Phytologist © 2021 New Phytologist Foundation

14698137, 2021, 2, Downloaded from https://nph.onlinelibrary.wiley.com/doi/10.1111/nph.17403 by Zhejiang Agr & For University, Wiley Online Library on [17/10/2023]. See the Terms and Conditions (https://onlinelibrary.wiley.com/terms-and-conditions) on Wiley Online Library for rules of use; OA articles are governed by the applicable Creative Commons License

14698137, 2021, 2, Downloaded from https://nph.onlinelibrary.wiley.com/doi/10.1111/nph.17403 by Zhejiang Agr & For University, Wiley Online Library on [17/10/2023]. See the Terms and Conditions (https://onlinelibrary.wiley.com/terms-and-conditions) on Wiley Online Library for rules of use; OA articles are governed by the applicable Creative Commons License

which in turn promotes its transphosphorylation (Gleason *et al.*, 2006; Miller *et al.*, 2013; Routray *et al.*, 2013). The target substrates of CCaMK, CIP73, IPD3/CYCLOPS and NAC84 are also gradually identified (Yano *et al.*, 2008; Kang *et al.*, 2011; Zhu *et al.*, 2016). However, the upstream factor affecting Ca^{2+} binding and autophosphorylation of CCaMK is largely unknown. Because $ZmCCaMK^{S67D}$ displays a much faster electrophoretic mobility and an enhanced Ca^{2+}-binding ability, in contrast with the situation of $ZmCCaMK^{S67A}$ (Fig. 7a,b), it becomes clear that the phosphorylation of Ser-67 promotes the binding of ZmCCaMK to Ca^{2+}. Following up on this, we further find that Ser-67 phosphorylation of ZmCCaMK significantly increases its autophosphorylation activity (Fig. 5a,c). Therefore, as a novel upstream factor, ZmBSK1 phosphorylates ZmCCaMK in Ser-67, which promotes ZmCCaMK binding to Ca^{2+} and enhances ZmCCaMK autophosphorylation. The next important step for CCaMK activation is CaM binding. The activation of some autophosphorylation sites of CCaMK regulates its Ca^{2+}/CaM-binding ability, thus affecting its kinase activity. The autophosphorylation at conserved sites Thr-271 in *Medicago truncatula* CCaMK (or Thr-265 in *Lotus japonicas* CCaMK, Thr-267 in *Lilium longiflorum* CCaMK or Thr-263 in *Oryza sativa* CCaMK) and Ser-343/Ser-344 play positive or negative roles in regulating CCaMK activity (Singh & Parniske, 2012; Miller *et al.*, 2013; Poovaiah *et al.*, 2013; Routray *et al.*, 2013; Ni *et al.*, 2019). Thr-271 autophosphorylation stimulates CCaMK activation (Poovaiah *et al.*, 2013) and Thr-263 autophosphorylation is required for the activation of OsDMI3 (Ni *et al.*, 2019). However, the phosphorylation at Ser-343 and Ser-344 is found to be associated with the negative regulation of CCaMK (Liao *et al.*, 2012; Routray *et al.*, 2013). These findings suggest the complexity in the regulation mechanism of CCaMK activation. In the current study, Ser-67 phosphorylation of ZmCCaMK indeed exhibited stronger binding ability to ZmCaM1 and higher transphosphorylation activity (Figs 5b,d, 7c,d). We thus propose that Ser-67 phosphorylation enhances the binding of ZmCCaMK to Ca^{2+} and CaM, and in turn increases both autophosphorylation activity and transphosphorylation activity of ZmCCaMK (Figs 5, 7). However, a more detailed molecular mechanism for understanding CCaMK activation is still critical.

Besides the signal transduction, alternative splicing (AS) events have been revealed to modulate plant abiotic stress tolerance. In maize, Li *et al.* (2019) found that several *BSKs* have diverse splicing transcripts, which are expressed in different tissues and respond to various stimuli, indicating a novel post-transcriptional regulation pattern in *BSK* genes. Sequential window acquisition of all theoretical fragment ion spectra MS (SWATH-MS) has emerged to detect AS and quantify proteome dynamics (Blank-Landeshammer *et al.*, 2019; Chen *et al.*, 2020a,b, 2021a,b; Zhu *et al.*, 2020). Using OE-*ZmBSK1* and RNAi-*ZmBSK1* transgenic lines, we would like to find more targets that are regulated by ZmBSK1 through SWATH-MS and transcriptome analysis in future. Moreover, transgenic maize plants overexpressing AS variants of *BSKs* will be generated to investigate whether the AS of *BSKs* modulate maize drought tolerance.

Acknowledgements

This study was supported by grants from the National Natural Science Foundation of China (31671603, 31871534 and 32001445) and the China Postdoctoral Science Foundation (2019M651846). We thank Prof. Yiqun Bao (Nanjing Agriculture University) for providing 1300-221-3*Flag and 1300-221-6*Myc vectors.

Author contributions

AZ conceived the project. AZ and LL designed the experiments. LL performed most of the experiments and analyzed the data. YX, JY, PD, JL, XS and GH performed some of the experiments. AZ and LL wrote the manuscript. JY, MJ, LN, JY and YX revised the manuscript.

ORCID

Lei Liu https://orcid.org/0000-0002-6388-2077
Yang Xiang https://orcid.org/0000-0001-7920-7554
Jingwei Yan https://orcid.org/0000-0003-4930-0875
Aying Zhang https://orcid.org/0000-0003-3779-1603

References

Ahammed GJ, Ruan YP, Zhou J, Xia XJ, Shi K, Zhou YH, Yu JQ. 2013. Brassinosteroid alleviates polychlorinated biphenyls-induced oxidative stress by enhancing antioxidant enzymes activity in tomato. *Chemosphere* **90**: 2645–2653.

Anjum SA, Wang LC, Farooq M, Hussain M, Xue LL, Zou CM. 2011. Brassinolide application improves the drought tolerance in maize through modulation of enzymatic antioxidants and leaf gas exchange. *Journal of Agronomy and Crop Science* **197**: 177–185.

Arazi T, Baum G, Snedden WA, Shelp BJ, Fromm H. 1995. Molecular and biochemical analysis of calmodulin interactions with the calmodulin-binding domain of plant glutamate decarboxylase. *Plant Physiology* **108**: 551–561.

Bayer M, Nawy T, Giglione C, Galli M, Meinnel T, Lukowitz W. 2009. Paternal control of embryonic patterning in *Arabidopsis thaliana*. *Science* **323**: 1485–1488.

Blank-Landeshammer B, Teichert I, Marker R, Nowrousian M, Kuck U, Sickmann A. 2019. Combination of proteogenomics with peptide de novo sequencing identifies new genes and hidden posttranscriptional modifications. *mBio* **10**: e02367–e2419.

Boutraa T, Akhkha A, Al-Shoaibi AA, Alhejeli AM. 2010. Effect of water stress on growth and water use efficiency (WUE) of some wheat cultivars (*Triticum durum*) grown in Saudi Arabia. *Journal of Taibah University for Science* **3**: 39–48.

Bradford MM. 1976. A rapid and sensitive method for the quantitation of microgram quantities of protein utilizing the principle of protein-dye binding. *Analytical Biochemistry* **72**: 248–254.

Chai Q, Gan YT, Zhao C, Xu HL, Waskom RM, Niu YN, Siddique KHM. 2016. Regulated deficit irrigation for crop production under drought stress. A review. *Agronomy for Sustainable Development* **36**: 3.

Chen G, Wang Y, Wang X, Yang Q, Quan X, Zeng J, Dai F, Zeng F, Wu F, Zhang G *et al.* 2019. Leaf epidermis transcriptome reveals drought-induced hormonal signaling for stomatal regulation in wild barley. *Plant Growth Regulation* **87**: 39–54.

Chen H, Zou Y, Shang Y, Lin H, Wang Y, Cai R, Tang X, Zhou JM. 2008. Firefly luciferase complementation imaging assay for protein-protein interactions in plants. *Plant Physiology* **146**: 368–376.

Chen M-X, Lu C-C, Sun P-C, Nie Y-X, Tian Y, Hu Q-J, Das D, Hou X-X, Gao B, Chen Xi *et al.* 2021a. Comprehensive transcriptome and proteome analyses

© 2021 The Authors
New Phytologist © 2021 New Phytologist Foundation

reveal a novel sodium chloride responsive gene network in maize seed tissues during germination. *Plant, Cell & Environment* **44**: 88–101.

Chen MX, Mei LC, Wang F, Boyagane Dewayalage IKW, Yang JF, Dai L, Yang GF, Gao B, Cheng CL, Liu YG. 2021b. PlantSPEAD: a web resource towards comparatively analysing stress-responsive expression of splicing-related proteins in plant. *Plant Biotechnology Journal* **19**: 227–229.

Chen MX, Zhang Y, Fernie AR, Liu YG, Zhu FY. 2020a. SWATH-MS-Based Proteomics: strategies and applications in plants. *Trends in Biotechnology* **39**: 433–437.

Chen M-X, Zhu F-Y, Gao B, Ma K-L, Zhang Y, Fernie AR, Chen Xi, Dai L, Ye N-H, Zhang X *et al.* 2020b. Full-length transcript-based proteogenomics of rice improves its genome and proteome annotation. *Plant Physiology* **182**: 1510–1526.

Cruz de Carvalho MH. 2008. Drought stress and reactive oxygen species: production, scavenging and signaling. *Plant Signaling & Behavior* **3**: 156–165.

Diedhiou I, Diouf D. 2018. Transcription factors network in root endosymbiosis establishment and development. *World Journal of Microbiology and Biotechnology* **34**: 37.

Duan M, Zhang RX, Zhu FG, Zhang ZQ, Gou LM, Wen JQ, Dong JL, Wang T. 2017. A lipid-anchored NAC transcription factor is translocated into the nucleus and activates glyoxalase I expression during drought stress. *The Plant Cell* **29**: 1748–1772.

Farooq M, Wahid A, Basra SMA, Islam-ud-Din. 2009. Improving water relations and gas exchange with brassinosteroids in rice under drought stress. *Journal of Agronomy and Crop Science* **195**: 262–269.

Gampala SS, Kim T-W, He J-X, Tang W, Deng Z, Bai M-Y, Guan S, Lalonde S, Sun Y, Gendron JM *et al.* 2007. An essential role for 14-3-3 proteins in brassinosteroid signal transduction in *Arabidopsis*. *Development Cell* **13**: 177–189.

Gleason C, Chaudhuri S, Yang T, Munoz A, Poovaiah BW, Oldroyd GE. 2006. Nodulation independent of rhizobia induced by a calcium-activated kinase lacking autoinhibition. *Nature* **441**: 1149–1152.

Hayashi T, Banba M, Shimoda Y, Kouchi H, Hayashi M, Imaizumi-Anraku H. 2010. A dominant function of CCaMK in intracellular accommodation of bacterial and fungal endosymbionts. *The Plant Journal* **63**: 141–154.

Hayat S, Khalique G, Wani AS, Alyemeni MN, Ahmad A. 2014. Protection of growth in response to 28-homobrassinolide under the stress of cadmium and salinity in wheat. *International Journal of Biological Macromolecules* **64**: 130–136.

Jia Z, Giehl RFH, Meyer RC, Altmann T, von Wiren N. 2019. Natural variation of BSK3 tunes brassinosteroid signaling to regulate root foraging under low nitrogen. *Nature Communications* **10**: 2378.

Jiang M, Zhang J. 2002. Water stress-induced abscisic acid accumulation triggers the increased generation of reactive oxygen species and up-regulates the activities of antioxidant enzymes in maize leaves. *Journal of Experimental Botany* **53**: 2401–2410.

Jin Y, Liu H, Luo D, Yu N, Dong W, Wang C, Zhang X, Dai H, Yang J, Wang E. 2016. DELLA proteins are common components of symbiotic rhizobial and mycorrhizal signalling pathways. *Nature Communications* **7**: 12433.

Kang H, Zhu H, Chu X, Yang Z, Yuan S, Yu D, Wang C, Hong Z, Zhang Z. 2011. A novel interaction between CCaMK and a protein containing the Scythe_N ubiquitin-like domain in *Lotus japonicus*. *Plant Physiology* **155**: 1312–1324.

Kato M, Watanabe Y, Iino S, Takaoka Y, Kobayashi S, Haga T, Hidaka H. 1998. Cloning and expression of a cDNA encoding a new neurocalcin isoform (neurocalcin α) from bovine brain. *Biochemical Journal* **331**: 871–876.

Kaya C, Ashraf M, Wijaya L, Ahmad P. 2019. The putative role of endogenous nitric oxide in brassinosteroid-induced antioxidant defence system in pepper (*Capsicum annuum* L.) plants under water stress. *Plant Physiology and Biochemistry* **143**: 119–128.

Kim TW, Guan S, Sun Y, Deng Z, Tang W, Shang JX, Sun Y, Burlingame AL, Wang ZY. 2009. Brassinosteroid signal transduction from cell-surface receptor kinases to nuclear transcription factors. *Nature Cell Biology* **11**: 1254–1260.

Kim TW, Wang ZY. 2010. Brassinosteroid signal transduction from receptor kinases to transcription factors. *Annual Review of Plant Biology* **61**: 681–704.

Levy J, Bres C, Geurts R, Chalhoub B, Kulikova O, Duc G, Journet EP, Ane JM, Lauber E, Bisseling T *et al.* 2004. A putative Ca^{2+} and calmodulin-dependent protein kinase required for bacterial and fungal symbioses. *Science* **303**: 1361–1364.

Li Z, Shen J, Liang J. 2019. Genome-wide identification, expression profile, and alternative splicing analysis of the brassinosteroid-signaling kinase (BSK) family genes in *Arabidopsis*. *International Journal of Molecular Sciences* **20**: 1138.

Li ZY, Xu ZS, He GY, Yang GX, Chen M, Li LC, Ma YZ. 2012. A mutation in *Arabidopsis BSK5* encoding a brassinosteroid-signaling kinase protein affects responses to salinity and abscisic acid. *Biochemical and Biophysical Research Communications* **426**: 522–527.

Liao J, Singh S, Hossain MS, Andersen SU, Ross L, Bonetta D, Zhou Y, Sato S, Tabata S, Stougaard J *et al.* 2012. Negative regulation of CCaMK is essential for symbiotic infection. *The Plant Journal* **72**: 572–584.

Liu YB, Qin LJ, Han LZ, Xiang Y, Zhao DG. 2015. Overexpression of maize *SDD1* (*ZmSDD1*) improves drought resistance in *Zea mays* L. by reducing stomatal density. *Plant Cell, Tissue and Organ Culture* **122**: 147–159.

Ma F, Lu R, Liu H, Shi B, Zhang J, Tan M, Zhang A, Jiang M. 2012. Nitric oxide-activated calcium/calmodulin-dependent protein kinase regulates the abscisic acid-induced antioxidant defence in maize. *Journal of Experimental Botany* **63**: 4835–4847.

Majhi BB, Sreeramulu S, Sessa G. 2019. BRASSINOSTEROID-SIGNALING KINASE5 associates with immune receptors and is required for immune responses. *Plant Physiology* **180**: 1166–1184.

Miller JB, Pratap A, Miyahara A, Zhou L, Bornemann S, Morris RJ, Oldroyd GE. 2013. Calcium/Calmodulin-dependent protein kinase is negatively and positively regulated by calcium, providing a mechanism for decoding calcium responses during symbiosis signaling. *The Plant Cell* **25**: 5053–5066.

Mitra RM, Gleason CA, Edwards A, Hadfield J, Downie JA, Oldroyd GE, Long SR. 2004. A Ca^{2+}/calmodulin-dependent protein kinase required for symbiotic nodule development: Gene identification by transcript-based cloning. *Proceedings of the National Academy of Sciences, USA* **101**: 4701–4705.

Neu A, Eilbert E, Asseck LY, Slane D, Henschen A, Wang K, Burgel P, Hildebrandt M, Musielak TJ, Kolb M *et al.* 2019. Constitutive signaling activity of a receptor-associated protein links fertilization with embryonic patterning in *Arabidopsis thaliana*. *Proceedings of the National Academy of Sciences, USA* **116**: 5795–5804.

Ni L, Fu X, Zhang H, Li X, Cai X, Zhang P, Liu L, Wang Q, Sun M, Wang QW *et al.* 2019. Abscisic acid inhibits rice protein phosphatase PP45 via H_2O_2 and relieves repression of the Ca^{2+}/CaM-dependent protein kinase DMI3. *The Plant Cell* **31**: 128–152.

Nolan TM, Vukasinovic N, Liu D, Russinova E, Yin Y. 2020. Brassinosteroids: multidimensional regulators of plant growth, development, and stress responses. *The Plant Cell* **32**: 295–318.

Pandey S, Tiwari SB, Tyagi W, Reddy MK, Upadhyaya KC, Sopory SK. 2002. A Ca^{2+}/CaM-dependent kinase from pea is stress regulated and *in vitro* phosphorylates a protein that binds to *AtCaM5* promoter. *European Journal of Biochemistry* **269**: 3193–3204.

Pimprikar P, Carbonnel S, Paries M, Katzer K, Klingl V, Bohmer M, Karl L, Floss D, Harrison M, Parniske M *et al.* 2016. A CCaMK-CYCLOPS-DELLA complex activates transcription of *RAM1* to regulate arbuscule branching. *Current Biology* **26**: 987–998.

Poovaiah BW, Du L, Wang H, Yang T. 2013. Recent advances in calcium/calmodulin-mediated signaling with an emphasis on plant-microbe interactions. *Plant Physiology* **163**: 531–542.

Porcel R, Barea JM, Ruiz-Lozano JM. 2003. Antioxidant activities in mycorrhizal soybean plants under drought stress and their possible relationship to the process of nodule senescence. *New Phytologist* **157**: 135–143.

Ren H, Willige BC, Jaillais Y, Geng S, Park MY, Gray WM, Chory J. 2019. BRASSINOSTEROID-SIGNALING KINASE 3, a plasma membrane-associated scaffold protein involved in early brassinosteroid signaling. *PLoS Genetics* **15**: e1007904.

Routray P, Miller JB, Du L, Oldroyd G, Poovaiah BW. 2013. Phosphorylation of S344 in the calmodulin-binding domain negatively affects CCaMK function during bacterial and fungal symbioses. *The Plant Journal* **76**: 287–296.

Sathyanarayanan PV, Cremo CR, Poovaiah BW. 2000. Plant chimeric Ca^{2+}/Calmodulin-dependent protein kinase. Role of the neural visinin-like domain in regulating autophosphorylation and calmodulin affinity. *Journal of Biological Chemistry* **275**: 30417–30422.

© 2021 The Authors
New Phytologist © 2021 New Phytologist Foundation

14698137, 2021, 2, Downloaded from https://nph.onlinelibrary.wiley.com/doi/10.1111/nph.17403 by Zhejiang Agr & For University, Wiley Online Library on [17/10/2023]. See the Terms and Conditions (https://onlinelibrary.wiley.com/terms-and-conditions) on Wiley Online Library for rules of use; OA articles are governed by the applicable Creative Commons License

Shi B, Ni L, Zhang A, Cao J, Zhang H, Qin T, Tan M, Zhang J, Jiang M. 2012. OsDMI3 is a novel component of abscisic acid signaling in the induction of antioxidant defense in leaves of rice. *Molecular Plant* **5**: 1359–1374.

Shi H, Shen Q, Qi Y, Yan H, Nie H, Chen Y, Zhao T, Katagiri F, Tang D. 2013. BR-SIGNALING KINASE1 physically associates with FLAGELLIN SENSING2 and regulates plant innate immunity in *Arabidopsis*. *The Plant Cell* **25**: 1143–1157.

Shimoda Y, Han L, Yamazaki T, Suzuki R, Hayashi M, Imaizumi-Anraku H. 2012. Rhizobial and fungal symbioses show different requirements for calmodulin binding to calcium calmodulin-dependent protein kinase in *Lotus japonicus*. *The Plant Cell* **24**: 304–321.

Shiu SH, Karlowski WM, Pan R, Tzeng YH, Mayer KF, Li WH. 2004. Comparative analysis of the receptor-like kinase family in *Arabidopsis* and rice. *The Plant Cell* **16**: 1220–1234.

Singh S, Katzer K, Lambert J, Cerri M, Parniske M. 2014. CYCLOPS, a DNA-binding transcriptional activator, orchestrates symbiotic root nodule development. *Cell Host & Microbe* **15**: 139–152.

Singh S, Parniske M. 2012. Activation of calcium- and calmodulin-dependent protein kinase (CCaMK), the central regulator of plant root endosymbiosis. *Current Opinion in Plant Biology* **15**: 444–453.

Sreeramulu S, Mostizky Y, Sunitha S, Shani E, Nahum H, Salomon D, Hayun LB, Gruetter C, Rauh D, Ori N *et al.* 2013. BSKs are partially redundant positive regulators of brassinosteroid signaling in *Arabidopsis*. *The Plant Journal* **74**: 905–919.

Takeda N, Maekawa T, Hayashi M. 2012. Nuclear-localized and deregulated calcium- and calmodulin-dependent protein kinase activates rhizobial and mycorrhizal responses in *Lotus japonicus*. *The Plant Cell* **24**: 810–822.

Tang W, Kim TW, Oses-Prieto JA, Sun Y, Deng Z, Zhu S, Wang R, Burlingame AL, Wang ZY. 2008. BSKs mediate signal transduction from the receptor kinase BRI1 in *Arabidopsis*. *Science* **321**: 557–560.

Thompson GA Jr, Okuyama H. 2000. Lipid-linked proteins of plants. *Progress in Lipid Research* **39**: 19–39.

Tirichine L, Imaizumi-Anraku H, Yoshida S, Murakami Y, Madsen LH, Miwa H, Nakagawa T, Sandal N, Albrektsen AS, Kawaguchi M *et al.* 2006. Deregulation of a Ca^{2+}/calmodulin-dependent kinase leads to spontaneous nodule development. *Nature* **441**: 1153–1156.

Vallone R, La Verde V, D'Onofrio M, Giorgetti A, Dominici P, Astegno A. 2016. Metal binding affinity and structural properties of calmodulin-like protein 14 from *Arabidopsis thaliana*. *Protein Science* **25**: 1461–1471.

Vardhini BV, Anjum NA. 2015. Brassinosteroids make plant life easier under abiotic stresses mainly by modulating major components of antioxidant defense system. *Frontiers in Environmental Science* **2**: 67.

Wang J, Shi H, Zhou L, Peng C, Liu D, Zhou X, Wu W, Yin J, Qin H, Ma W *et al.* 2017. OsBSK1-2, an orthologous of AtBSK1, is involved in rice immunity. *Frontiers in Plant Science* **8**: 908.

Xia XJ, Wang YJ, Zhou YH, Tao Y, Mao WH, Shi K, Asami T, Chen Z, Yu JQ. 2009. Reactive oxygen species are involved in brassinosteroid-induced stress tolerance in cucumber. *Plant Physiology* **150**: 801–814.

Xu J, Duan X, Yang J, Beeching JR, Zhang P. 2013. Enhanced reactive oxygen species scavenging by overproduction of superoxide dismutase and catalase delays postharvest physiological deterioration of cassava storage roots. *Plant Physiology* **161**: 1517–1528.

Yan H, Zhao Y, Shi H, Li J, Wang Y, Tang D. 2018. BRASSINOSTEROID-SIGNALING KINASE1 phosphorylates MAPKKK5 to regulate immunity in *Arabidopsis*. *Plant Physiology* **176**: 2991–3002.

Yan J, Guan L, Sun Y, Zhu Y, Liu L, Lu R, Jiang M, Tan M, Zhang A. 2015. Calcium and ZmCCaMK are involved in brassinosteroid-induced antioxidant defense in maize leaves. *Plant and Cell Physiology* **56**: 883–896.

Yang C, Li A, Zhao Y, Zhang Z, Zhu Y, Tan X, Geng S, Guo H, Zhang X, Kang Z *et al.* 2010. Overexpression of a wheat CCaMK gene reduces ABA sensitivity of *Arabidopsis thaliana* during seed germination and seedling growth. *Plant Molecular Biology Reporter* **29**: 681–692.

Yang L, Ji W, Zhu Y, Gao P, Li Y, Cai H, Bai X, Guo D. 2010. GsCBRLK, a calcium/calmodulin-binding receptor-like kinase, is a positive regulator of plant tolerance to salt and ABA stress. *Journal of Experimental Botany* **61**: 2519–2533.

Yang X, Zhao T, Rao P, Gao K, Yang X, Chen Z, An X. 2019. Transcriptome profiling of *Populus tomentosa* under cold stress. *Industrial Crops and Products* **135**: 283–293.

Yano K, Yoshida S, Muller J, Singh S, Banba M, Vickers K, Markmann K, White C, Schuller B, Sato S *et al.* 2008. CYCLOPS, a mediator of symbiotic intracellular accommodation. *Proceedings of the National Academy of Sciences, USA* **105**: 20540–20545.

Zhang A, Jiang M, Zhang J, Tan M, Hu X. 2006. Mitogen-activated protein kinase is involved in abscisic acid-induced antioxidant defense and acts downstream of reactive oxygen species production in leaves of maize plants. *Plant Physiology* **141**: 475–487.

Zhang A, Zhang J, Ye N, Cao J, Tan M, Zhang J, Jiang M. 2010. ZmMPK5 is required for the NADPH oxidase-mediated self-propagation of apoplastic H_2O_2 in brassinosteroid-induced antioxidant defence in leaves of maize. *Journal of Experimental Botany* **61**: 4399–4411.

Zhang A, Zhang J, Zhang J, Ye N, Zhang H, Tan M, Jiang M. 2011. Nitric oxide mediates brassinosteroid-induced ABA biosynthesis involved in oxidative stress tolerance in maize leaves. *Plant and Cell Physiology* **52**: 181–192.

Zhang B, Wang X, Zhao Z, Wang R, Huang X, Zhu Y, Yuan Li, Wang Y, Xu X, Burlingame AL *et al.* 2016. OsBRI1 activates BR signaling by preventing binding between the TPR and kinase domains of OsBSK3 via phosphorylation. *Plant Physiology* **170**: 1149–1161.

Zhu FY, Song YC, Zhang KL, Chen X, Chen MX. 2020. Quantifying plant dynamic proteomes by SWATH-based mass spectrometry. *Trends in Plant Science* **25**: 1171–1172.

Zhu Y, Yan J, Liu W, Liu L, Sheng Y, Sun Y, Li Y, Scheller HV, Jiang M, Hou X *et al.* 2016. Phosphorylation of a NAC transcription factor by a Calcium/Calmodulin-dependent protein kinase regulates abscisic acid-induced antioxidant defense in maize. *Plant Physiology* **171**: 1651–1664.

Supporting Information

Additional Supporting Information may be found online in the Supporting Information section at the end of the article.

Fig. S1 Specificity of polyclonal anti-ZmBSK1 and anti-ZmCCaMK antibodies.

Fig. S2 Subcellular localization and colocalization of ZmCCaMK and ZmBSK1 in maize.

Fig. S3 The kinase activities of ZmBSK1 and ZmCCaMK in the presence of Mn^{2+} or Ca^{2+}/CaM.

Fig. S4 The kinase activity of ZmBSK1 in maize plants exposed to PEG treatment.

Fig. S5 The expression levels and protein abundances of ZmBSK1, ZmCCaMK, ZmCCaMK^{S67A} and ZmCCaMK^{S67D} in transgenic maize plants.

Fig. S6 Overexpression and knockdown of *ZmBSK1* does not affect the expression levels of its homologous genes.

Fig. S7 The conserved ATP binding site in the kinase domain of plant CCaMKs and BSK protein.

Fig. S8 Specificity analysis of anti-pSer67-ZmCCaMK antibody.

© 2021 The Authors
New Phytologist © 2021 New Phytologist Foundation

14698137, 2021, 2, Downloaded from https://nph.onlinelibrary.wiley.com/doi/10.1111/nph.17403 by Zhejiang Agr & For University, Wiley Online Library on [17/10/2023]. See the Terms and Conditions (https://onlinelibrary.wiley.com/terms-and-conditions) on Wiley Online Library for rules of use; OA articles are governed by the applicable Creative Commons License

Fig. S9 Phylogenic analysis of BSK-related proteins in maize, *Arabidopsis* and rice.

Fig. S10 Subcellular localization of ZmBSK1^{G2A} in maize.

Methods S1 Bimolecular fluorescence complementation (BiFC) assay.

Methods S2 Expression and purification of recombinant proteins.

Methods S3 Western blot analysis.

Methods S4 *In vitro* synthesis of dsRNA.

Methods S5 Protoplast preparation and transfection with constructs or dsRNAs.

Methods S6 Subcellular localization and colocalization.

Methods S7 Cell fraction analysis.

Methods S8 Site-directed mutagenesis.

Methods S9 Phylogenetic analysis.

Methods S10 Accession numbers.

Table S1 Primers used in this study.

Table S2 Autophosphorylation sites of ZmCCaMK were identified by LC-MS/MS in this study.

Table S3 Total phosphorylation sites of ZmCCaMK were identified in the presence of ZmBSK1 by LC-MS/MS in this study.

Please note: Wiley Blackwell are not responsible for the content or functionality of any Supporting Information supplied by the authors. Any queries (other than missing material) should be directed to the *New Phytologist* Central Office.

About *New Phytologist*

- *New Phytologist* is an electronic (online-only) journal owned by the New Phytologist Foundation, a **not-for-profit organization** dedicated to the promotion of plant science, facilitating projects from symposia to free access for our Tansley reviews and Tansley insights.
- Regular papers, Letters, Viewpoints, Research reviews, Rapid reports and both Modelling/Theory and Methods papers are encouraged. We are committed to rapid processing, from online submission through to publication 'as ready' via *Early View* – our average time to decision is <26 days. There are **no page or colour charges** and a PDF version will be provided for each article.
- The journal is available online at Wiley Online Library. Visit **www.newphytologist.com** to search the articles and register for table of contents email alerts.
- If you have any questions, do get in touch with Central Office (np-centraloffice@lancaster.ac.uk) or, if it is more convenient, our USA Office (np-usaoffice@lancaster.ac.uk)
- For submission instructions, subscription and all the latest information visit **www.newphytologist.com**

© 2021 The Authors
New Phytologist © 2021 New Phytologist Foundation

14698137, 2021, 2, Downloaded from https://nph.onlinelibrary.wiley.com/doi/10.1111/nph.17403 by Zhejiang Agr & For University, Wiley Online Library on [17/10/2023]. See the Terms and Conditions (https://onlinelibrary.wiley.com/terms-and-conditions) on Wiley Online Library for rules of use; OA articles are governed by the applicable Creative Commons License